

Table 1. APL patients treated with As₂O₃ at Nagoya University Hospital

No.	Age, y	Sex	Diagnosis	Treatments prior to As ₂ O ₃	Disease status at As ₂ O ₃	Treatments after As ₂ O ₃	Outcome	Survival after As ₂ O ₃	As ₂ O ₃ resistance
1	61	M	M3v	A+CT	Rel1	(-)	D	6 y, 1 mo	+
2	35	M	M3	A+CT	Rel1	sib-PBSCT	A	3 y, 8 mo	-
3	30	M	M3	A+CT	Rel2	auto-PBSCT	A	6 y, 9 mo	-
4	41	M	M3	A+CT	Rel1	auto-PBSCT	A	5 y, 8 mo	-
5	62	M	M3	A+CT, HD-Ara-C	Rel3	CBT	D	10 mo	-
6	42	F	M3	A+CT, aPBSCT	Rel2	CBT	D	4 mo	+
7	46	F	M3	A+CT	2nd CR	auto-PBSCT	A	6 y, 7 mo	-
8	54	F	M3	A+CT	Rel2	auto-PBSCT	A	5 y, 9 mo	-
9	19	M	M3	A+CT	Rel1	UR-BMT	A	6 y, 1 mo	-
10	42	M	M3	A+CT, UR-BMT	Rel3	DLI	A	6 y	-
11	61	M	M3v	A+CT	Rel1	(-)	D	4 mo	-
12	48	M	M3	A+CT, HD-Ara-C	Rel2	auto-PBSCT	A	4 y, 9 mo	-
13	39	M	M3v	A+CT, UR-BMT	Rel3	CBT	D	5 mo	-
14	20	M	M3	A+CT	Rel1	auto-PBSCT	A	4 y, 9 mo	-
15	36	M	M3	A+CT	Rel1	auto-PBSCT	A	4 y, 2 mo	-

Fifteen patients were treated with As₂O₃ at Nagoya University Hospital during the period of January 2000–December 2008. Outcomes were confirmed on December 1, 2009. Patients 5, 6, and 13 received cord blood transplantation after As₂O₃. Patients 5 and 13 died of complications of transplantation without any relapse sign. Patient 6 died of relapse just after transplantation. Patient 11 died of brain bleeding due to APL relapse with disseminated intravascular coagulation.

Rel1 through 3 indicates the first to third relapse; A+CT, ATRA with combination chemotherapy; PBSCT, peripheral blood stem cell transplantation; CBT, cord blood transplantation; BMT, bone marrow transplantation; D, dead; and A, alive.

after treatment with chemotherapy with ATRA were treated with As₂O₃ (Table 1). The diagnosis of APL and its relapse were confirmed by bone marrow morphology according to the FAB classification, chromosomal abnormality t(15;17) in peripheral blood and/or bone marrow cells, positive RT-PCR assay for *PML-RARA* transcripts, and/or FISH analysis of *PML* and *RARA*. As₂O₃ was diluted in 500 mL of 5% dextrose and administered intravenously over 2 hours at a dose of 0.15 mg/kg daily for a cumulative maximum of 60 days.

Patient 1 (Table 1 and Figure 1A) was diagnosed with APL (the microgranular variant M3v) in October 1998 (Figure 1A), and complete remission (CR) was obtained after combination chemotherapy with ATRA (45 mg/m²/d). However, relapse with insufficient response to ATRA was observed (Figure 1A) after the end of consolidation therapy in August 1999. As₂O₃ (0.15 mg/kg/d) was started as a salvage chemotherapy, and a molecular response was obtained. The effectiveness of As₂O₃ gradually decreased during the patient's 7-year clinical course. Am80 (6 mg/m²/d) was started in July 2005 in addition to As₂O₃ therapy. However, the effectiveness was poor, and Am80 was discontinued in October 2005. Thereafter, only As₂O₃ was used. At the terminal stage of his clinical course (Figure 1A), As₂O₃ was administered under the condition that > 90% of his peripheral blood cells were considered APL blast cells, but no response to the elevated blast count was observed. We diagnosed this condition as secondary As₂O₃ resistance. The patient died of disease progression in January 2006. During his 7-year clinical course, clinical samples from his bone marrow and/or peripheral blood were obtained repeatedly (Figure 1A).

Patient 6 was diagnosed with APL in January 2000, and CR was obtained after combination chemotherapy with ATRA. Relapse was observed in February 2002. After obtaining a second CR with combination chemotherapy, autologous peripheral blood stem cell transplantation was performed in October 2002. An early relapse was observed after transplantation in February 2003, and then As₂O₃ (0.15 mg/kg/d) was started. Partial cytoreduction was confirmed, but CR was not obtained. We diagnosed this condition as primary refractory disease to As₂O₃. As₂O₃ was used for 42 days and then discontinued. Cord blood transplantation was performed during non-CR, but the patient died of relapsed disease in July 2003. Genomic DNA was obtained from leukemia cells harvested 27 days after starting As₂O₃ therapy. Although the patient's bone marrow showed hypocellularity at this time, 97.1% of her marrow cells were positive for the *PML-RARA* fusion gene with FISH analysis.

Cell preparation from patients

After obtaining informed consent from each patient in accordance with the Declaration of Helsinki, the patients' primary cells were obtained from their

peripheral blood and/or bone marrow. All experiments were conducted with institutional review board approval from the Nagoya University School of Medicine. Mononuclear cells were separated with Ficoll Paque (GE Healthcare) and preserved with CP-1 (Kyokuto Pharmaceutical Industrial) in liquid nitrogen until further analysis.

RNA extraction and RT-PCR

Total RNA was isolated from each sample using TRIzol (Invitrogen). cDNA was synthesized from 5 μg of total RNA using Superscript II reverse transcriptase (Invitrogen) as described previously.^{26,27} PCR was performed using LA-Taq polymerase (Takara) under the following conditions: one cycle of 95°C for 4 minutes, followed by 40 cycles of 95°C for 30 seconds, 55°C for 30 seconds, and 72°C for 60 seconds. PCR primers for amplification of the coding sequences of *PML-RARA* are as follows: forward PR-U619: 5'-TGT TCC AAG CCG CTG T-3', reverse PR-L2189: 5'-CAT CTT CAG CGT GAT CA-3'. Amplified PCR fragments were purified with a Wizard PCR prep DNA purification kit (Promega) and cloned into the pCR2.1-TOPO cloning vector (Invitrogen). At least 20 clones were sequenced with an ABI 310 automated DNA sequencer (Applied Biosystems). Genetic mutations were confirmed using MacVector Version 10.5.1 software.

Expression vectors

The coding sequence of *PML-RARA* was amplified with PCR, and the Flag sequence was added with the forward primer as described previously.^{26,28} The PCR fragment was cloned into the pcDNA4-His-Max-TOPO mammalian expression vector (Invitrogen) to generate the following expression vectors: pcDNA4-XF-PR-WT for Xpress-tagged wild-type *PML-RARA*, pcDNA4-XF-PR-B/L-mut for Xpress-tagged *PML-RARA* with mutations resulting in A216V and G391E substitutions, pcDNA4-XF-PR-B2-mut for *PML-RARA* with the A216V substitution, and pcDNA4-XF-PR-L-B2-mut2 for the long-form *PML-RARA* with the L218P substitution. To express the long form of the wild-type *PML-RARA* protein, pcDNA4-XF-PR-L was used as described previously.²⁹ Expression vectors pcDNA-F-Ubc9, pcDNA-F-SUMO, and pcDNA-HA-PML for Flag-tagged Ubc9 and SUMO1, and HA-tagged PML, respectively, have also been described previously.³⁰

Cell culture

Cells of the human cervical cancer cell line HeLa were cultured in DMEM containing 10% FCS. U937 cells, a human monocytic leukemia cell line, were cultured in RPMI containing 10% FCS.

Protein extraction and antibodies for immunoblotting

HeLa cells (1.0×10^5 /well) were cultured in a 12-well plate for 12 hours before transfection. Transfection of the expression vectors was carried out using Effectene (Invitrogen) according to the manufacturer's instructions. The cells were washed with DMEM 24 hours after transfection, and then incubated for 8 hours with or without $10 \mu\text{M}$ As_2O_3 (Sigma-Aldrich) until protein extraction. Whole-cell protein samples for immunoblotting were obtained using 250 μL of Laemmli sample buffer (200mM Tris-HCl, pH 6.8, 4% SDS, 20% glycerol, 10% 2-mercaptoethanol, and 0.004% bromophenol blue). After boiling for 5 minutes, samples were subjected to SDS-PAGE.

U937 cells were cultured in a 12-well plate for 12 hours before transfection. Transfection of the expression vectors pcDNA4-XF-PR-WT and pcDNA4-XF-PR-B/L-mut was carried out using Nucleofector Kit C (Lonza) according to the manufacturer's instructions. After 12 hours, immunofluorescent analysis was performed.

To separate PML-RARA protein into soluble and/or insoluble fractions, cells were lysed in 200 μL of RIPA lysis buffer (50mM Tris-HCl, pH 7.5, 150mM NaCl, 1% NP-40, 0.5% sodium deoxycholate, 0.1% SDS, 0.2mM PMSF, and a complete mini protease inhibitor tablet [Roche]). After centrifugation at 10 000g for 10 minutes, the supernatants were placed into new tubes, and 200 μL of 2 \times SDS sample buffer was added (soluble fraction). PBS (20 μL) and 200 μL of 2 \times SDS sample buffer were added to the pellets (insoluble fraction). After boiling for 5 minutes, samples were analyzed by SDS-PAGE followed by immunoblotting. Antibodies used in this assay are as follows: rabbit anti-hemagglutinin (anti-HA; Sigma-Aldrich), mouse anti-Xpress tag (Invitrogen), and mouse anti-FLAG-M2 (Sigma-Aldrich).

Immunofluorescence microscopy

HeLa cells expressing Flag- and Xpress-tagged PML-RARA and its mutated proteins were cultured on Chamber Slides (Lab-Tek) with or without $10 \mu\text{M}$ As_2O_3 . U937 cells expressing Flag- and Xpress-tagged PML-RARA and its mutated proteins and the primary leukemia cells were placed on slide glasses using Cytospin (Shandon Southern Products), air dried, and fixed in acetone/methanol for 10 minutes at -20°C . Cells were then blocked with 1% BSA (Sigma-Aldrich) in PBS for 1 hour, incubated with primary antibodies for 3 hours, and incubated with Alexa Fluor 488 (green)- or 568 (red)-conjugated secondary antibodies for 1 hour at room temperature. Antibodies used in this assay are as follows: rabbit anti-human PML (Santa Cruz Biotechnology), mouse anti-FLAG-M2 (Sigma-Aldrich), rabbit Alexa Fluor 488 (Invitrogen), and mouse Alexa Fluor 568 (Invitrogen). The slides were examined with an Axioskop 2 fluorescence microscope (Carl Zeiss), photos were taken and analyzed with AxioVision FRET Release 4.5, and images were processed with Adobe Photoshop CS3 software.

Results

Two of 15 patients showed clinical As_2O_3 resistance

From January 2000 to December 2008 in Nagoya University Hospital, 15 relapsed patients with APL, including 3 with M3v ,³¹ were treated with As_2O_3 (Table 1). As a first-line treatment, combination chemotherapies with ATRA were administered to all patients. Thirteen patients received autologous or allogeneic stem cell transplantation after treatment with As_2O_3 , and long-term remission (range, 44-81 months) was confirmed in 10 patients. One patient (patient 1; see also "Patients") showed resistance to As_2O_3 after repeated therapy. Another patient (patient 6; see also "Patients") showed resistance to the first course of As_2O_3 therapy. Disease progression (elevation of the blast count in the peripheral blood) was observed in patient 1 after long-term treatment with As_2O_3 , and primary refractory disease that was resistant to As_2O_3 was confirmed in patient 6. Both patients died after disease progression.

Acquired missense mutations in PML-RARA transcripts observed in the 2 patients with As_2O_3 resistance

To determine the molecular mechanisms of the resistance to As_2O_3 , we first focused on patient 1 who had a long clinical course and whose clinical samples had been preserved several times at each disease stage.

Total RNA was extracted from each sample, and RT-PCR for PML-RARA transcripts was performed. DNA sequencing analysis using the sample obtained from the terminal stage was performed first (Figure 1A sample 5). The PML-RARA transcript was a short-form type (bcr3^{32}) that lacked the nuclear localizing signal (NLS) in PML. Missense mutations resulting in the A216V substitution in the PML-B2 domain and the G391E substitution in the RARA ligand-binding domain (LBD; Figure 1B) were detected. The predicted mutated PML-RARA protein resulting from these mutations is shown in Figure 2A.

We then determined the sequence of PML-RARA in patient #6, who showed primary refractory disease to As_2O_3 . Only a limited clinical sample obtained at 27 days after starting the As_2O_3 treatment was available for genomic analysis. A missense mutation resulting in an L218P substitution in the PML-B2 domain was confirmed in 2 of 20 clones with PCR cloning using genomic DNA PCR (Figure 1C). The mutations in the PML-B2 domain are indicated as B2-mut and B2-mut2 in Figure 1D. The predicted mutated PML-RARA protein designated as PR-L-B2-mut2 is also shown in Figure 2A. The location of these mutations is very close to the As_2O_3 -binding cysteine-cysteine (CC) motif reported by Jeanne et al.²⁵

Clonal expansion of PR-B/L-mut at the terminal stage of APL disease progression

To confirm the clonal expansion of the genetic mutations in PML-RARA, we performed sequencing analysis using the RT-PCR fragments of PML-RARA transcripts from the serial clinical samples obtained from patient 1 (samples 1-5 in Figure 1A). PCR fragments were cloned into the vector, and at least 20 clones were picked for sequencing analysis. Genetic mutations resulting in PR-B2-mut, PR-LBD-mut, and PR-B/L-mut (Figure 2A) were confirmed in samples 4 and 5 obtained at this patient's terminal stage when As_2O_3 resistance and the expansion of the blast count were clinically observed (Figure 2B). These clones were not confirmed in samples 1-3, and the partial response to As_2O_3 treatment was confirmed at the periods 2-3. The samples 2 and 3 had blasts showing FISH-positive PML-RARA clones (33.9% and 74.0%, respectively). This result strongly suggests that these mutations were closely related to disease progression during As_2O_3 treatment.

Lack of multimerization of PR-B/L-mut with and without As_2O_3

Posttranslational modification of PML, including SUMOylation, is reported to be critical for the responsiveness to As_2O_3 .^{24,25,33} To confirm the functional difference between PR-WT and its mutant, we performed an in vitro SUMOylation assay in HeLa cells. HA-tagged PML, Xpress-tagged PR-WT, PR-B/L-mut, and SUMO1/Ubc9 were expressed in HeLa cells with or without $10 \mu\text{M}$ As_2O_3 (Figure 3A-B). PML, PR-WT, and PR-B/L-mut were detected with immunoblotting. SUMO1/Ubc9 is coexpressed with PML, and therefore, SUMOylated PML bands were observed (indicated with black triangles in Figure 3A lane 2). The intensity of the mobility-shifted bands was increased with As_2O_3 treatment (Figure 3A lane 3). When using PR-WT, multimerized/SUMOylated

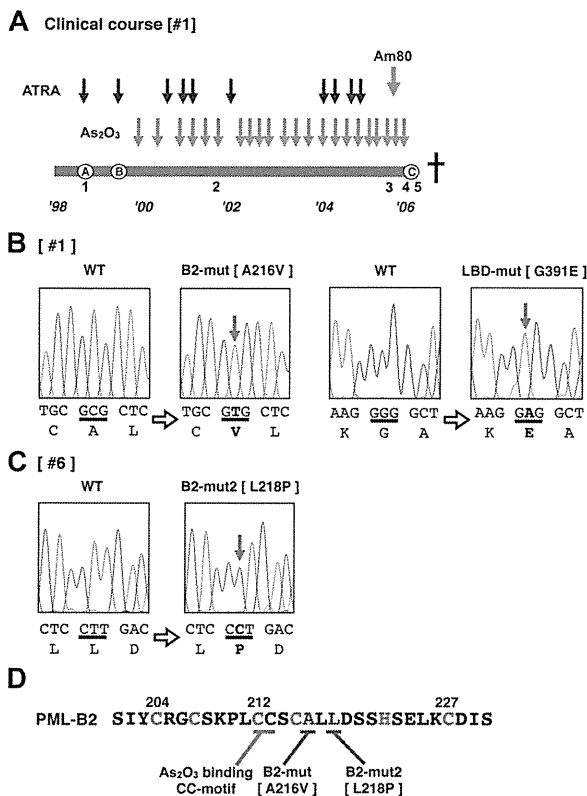


Figure 1. Additional genetic mutations in PML-RARA in patients showing an As₂O₃ refractory/resistant phenotype. (A) Clinical course of patient 1, who showed As₂O₃ resistance in the terminal stage of disease progression. The total clinical duration of the patient was almost 7 years. Detailed information is described in “Methods.” Black and gray arrows indicate the course of chemotherapies with ATRA, As₂O₃, and Am80. The letters A-C enclosed in circles indicate clinically important time points: A indicates diagnosis with APL, B indicates relapse with inadequate response to ATRA, and C indicates confirmation of clinical As₂O₃ resistance. This patient died of disease progression. Leukemia cells from the bone marrow and peripheral blood were obtained at time periods 1-5. Genetic mutations in PML-RARA were confirmed in patients 1 (B) and 6 (C). Missense point mutations in the PML B2 domain and RARA LBD domain were confirmed in the leukemia cells from time point 5. DNA sequences and the genetic code are indicated in capital letters. Bold letters indicate mutations. (D) The zinc finger motif of the PML-B2 domain. Amino acid substitutions in patients 1 and 6 are depicted. The CC motif critical for As₂O₃ binding²⁵ is also indicated. The “C” and “H” in red are the cysteine and histidine, respectively, which are important for zinc finger formation.

PR-WT bands were confirmed with and without As₂O₃ (Figure 3B lanes 4-6 black triangles). However, when using PR-B/L-mut, oligomerized/SUMOylated PML-RARA protein was not observed with SUMO1/Ubc9 with or without As₂O₃ (Figure 3B lanes 8 and 9). When PR-B2-mut was used in the same assay system, nearly the same result was obtained (Figure 3B lanes 11 and 12). These results indicate that the genetic mutation leading to amino acid alteration of the PML-B2 domain is critical for the appropriate posttranslational modification of the PML-RARA protein, including SUMOylation and oligomerization.

Distinct cellular localization of PR-WT and PR-B/L-mut in soluble/insoluble fractions

Recently, it has been reported that As₂O₃ promotes PML-RARA multimerization via disulfide-mediated covalent binding, leading to formation of PML nuclear bodies; these multimers are subsequently SUMOylated.²⁵ To confirm the cellular localization (soluble/insoluble fractions, see also “Methods”) of PML, PR-WT, and PR-B/L-mut with or without As₂O₃, we performed immunoblotting

using HeLa cells that were transiently overexpressing each protein. Cells were lysed using RIPA buffer, as described previously,^{14,24} and the whole-cell lysate was separated into 2 fractions, soluble (supernatant) and insoluble (pellet). In the absence of As₂O₃, PML was localized in both the soluble and insoluble fractions (Figure 4A lanes 1 and 3). With As₂O₃, PML was detected mostly in the insoluble fraction (Figure 4A lanes 2 and 4). Nearly the same results were obtained with PR-WT (short form of PML-RARA, Figure 4B lanes 5, 6, 11, and 12) and PR-long (long form of PML-RARA, Figure 4B lanes 9, 10, 15, and 16). Conversely, PR-B/L-mut was localized in both the soluble and insoluble fractions with and without As₂O₃, and protein modification including multimerization was not observed with this assay system (Figure 4B lanes 7, 8, 13, and 14). Protein expression levels were quantitated with BioMax software, and the relative intensity is depicted in Figure 4C. These findings indicate that As₂O₃ did not affect PR-B/L-mut compared with PML and PR-WT in this assay system, and this phenomenon was closely related to insufficient SUMOylation (Figure 3).

Distinct cellular localization of PR-WT and PR-B/L-mut with or without As₂O₃ in HeLa and U937 cells

We then performed immunofluorescent (IF) staining to examine the cellular localization pattern of wild-type PML, PR-WT, and PR-B/L-mut in HeLa cells (Figure 5). Wild-type PML was overexpressed in HeLa cells, which were incubated with or without As₂O₃. PML localization was confirmed by IF staining using an anti-PML antibody. PML was localized in PML nuclear bodies showing a speckled pattern without As₂O₃ (Figure 5Ai,iii). In the presence of As₂O₃, the localization pattern was clearly altered to a macrogranular pattern (Figure 5Aiv,vi).

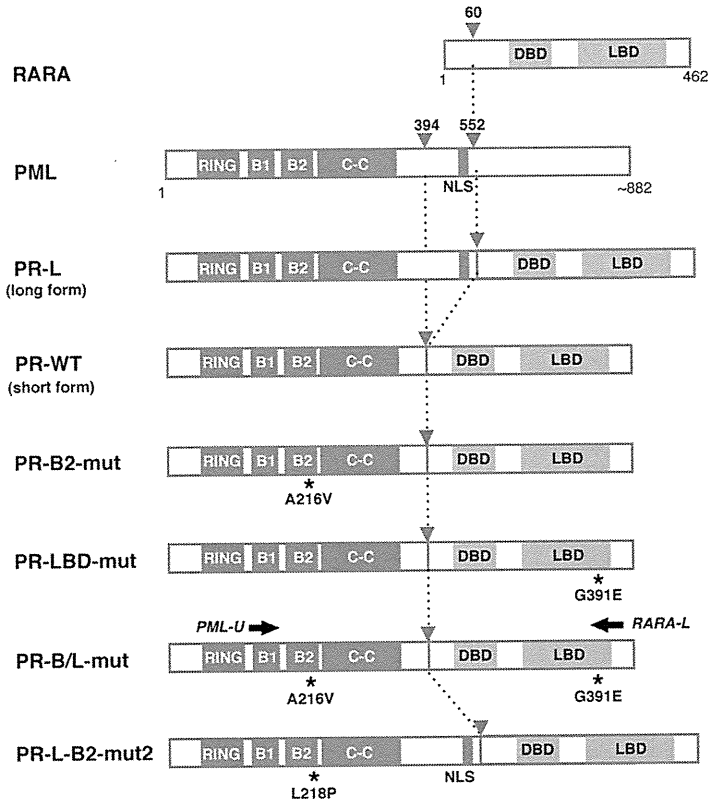
Similar analyses using PR-WT- and PR-B/L-mut-expressing HeLa cells were also performed (Figure 5B-C). Anti-PML antibody was used to detect endogenous PML, overexpressed PR-WT, and PR-B/L-mut, and anti-Flag antibody was used to detect PR-WT and PR-B/L-mut. In the absence of As₂O₃, PR-WT, a PML-RARA short form without an NLS, was detected around the nucleus as a microgranular pattern (Figure 5Bi,ii,iv), and as a macrogranular pattern in the presence of As₂O₃ (Figure 5Bv,vi, and viii). Surprisingly, PR-B/L-mut was localized differently in the cytoplasm as a diffuse pattern without As₂O₃ (Figure 5C,i,ii,iv), and the localization of PR-B/L-mut was not altered in the presence of As₂O₃ (Figure 5Cv,vi,viii). With As₂O₃ treatment, endogenous PML was confirmed in the nucleus with the macrogranular pattern (Figure 5Cv,viii). Transfected PR-B/L-mut (red fluorescence) could not be confirmed in the nucleus (Figure 5Cvi). The localization of PR-B2-mut showed almost the same pattern as PR-B/L-mut (data not shown). These data strongly suggest that the point mutation in the PML-B2 domain disrupts or inhibits PML body formation and the responsiveness to As₂O₃ treatment.

Nearly identical analyses using U937 cells were performed to confirm the significance in hematopoietic cells. As indicated in Figure 5D, PR-WT was observed in the cytoplasm with the microgranular pattern (Figure 5Di,ii,iv), and PR-B/L-mut showed a diffuse pattern, as observed in HeLa cells (Figure 5Dv,vi,viii).

Distinct cellular localization of PR-L and PR-L-B2-mut2 with or without As₂O₃ in HeLa cells

We also performed a similar analysis using PR-L and PR-L-B2-mut2 to show the molecular significance of the L218P mutation

A



B

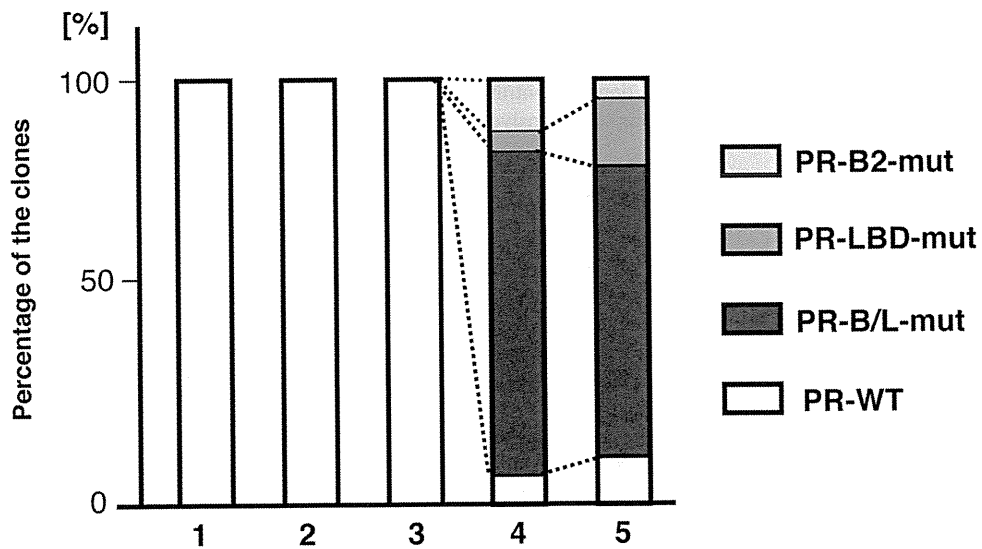


Figure 2. Clonal expansion of PML-B2 and RARA-LBD mutations during disease progression. (A) Schematic representation of PML, RARA, and its fusion proteins with or without mutations. Functional domains are indicated. Gray arrowheads indicate the break points of the fusion proteins. Black asterisks depict amino acid substitutions resulting from genetic mutations. Black arrows indicate the positions of the PCR primers for amplifying *PML-RARA* fusion transcripts. RING indicates the RING finger; B1 and B2, B-box motifs; C-C, coiled-coil; and DBD, DNA-binding domain. (B) Clonal expansion of *PML-RARA* mutants. Using the clinical samples obtained at time points 1-5 in Figure 1A, RT-PCR using PCR primers (PML-U and RARA-L in Figure 1A) followed by cloning was performed. At least 20 clones were sequenced for each sample. The percentages of the clones are depicted in the bar graph.

in the B2 domain confirmed in patient 6 (Figure 6). PR-L, a PML-RARA long form with an NLS, was detected in the nucleus as a microgranular pattern without As₂O₃ (Figure 6Ai,ii,iv) and as a

macrogranular pattern with As₂O₃ (Figure 6Av,vi,viii). In contrast, PR-L-B2-mut2 was localized in the nucleus as a diffuse pattern without As₂O₃ (Figure 6Bi,ii,iv). The localization was not altered in

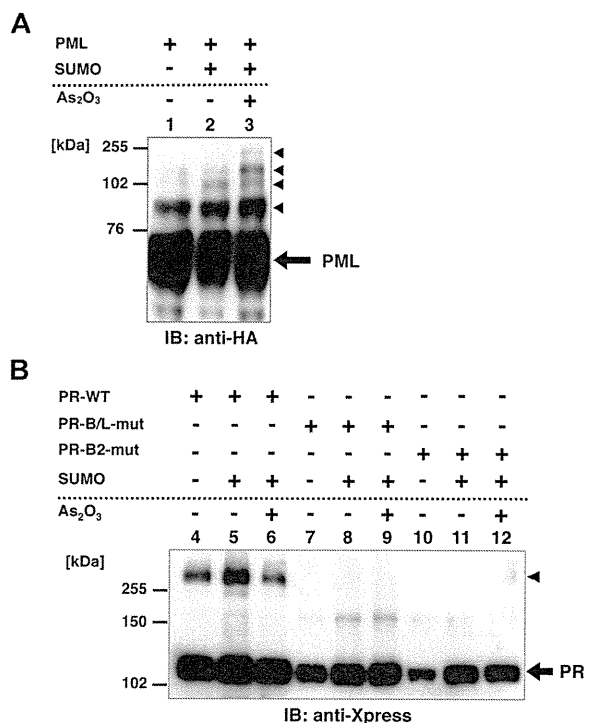


Figure 3. Posttranslational modification of PML, PR-WT, PR-B/L-mut, and PR-B2-mut induced by SUMO1/Ubc9. (A) HA-tagged PML and SUMO1/Ubc9 (SUMO) expression vectors were transfected into HeLa cells as indicated and incubated with or without As₂O₃ (10 μM) for 8 hours. Immunoblot analysis using an anti-HA antibody was carried out. Black arrowheads indicate SUMO-modified PML. (B) Xpress-tagged PR-WT, PR-B/L-mut, or PR-B2-mut was overexpressed in HeLa cells with or without SUMO1/Ubc9 and incubated with or without As₂O₃ (10 μM) for 8 hours. Black arrowhead indicates SUMO-modified/dimerized PR-WT (lanes 4-6). Note that the modified bands of PR-B/L-mut and PR-B2-mut were barely detected (lanes 7-12).

the presence of As₂O₃ (Figure 6Bv,vi,viii). These data strongly suggest that the L218P mutation in the PML-B2 domain contributes to the aberrant PML body formation and disrupts responsiveness to As₂O₃ treatment.

Cellular localization of endogenous PR-B/L-mut without As₂O₃ in primary cells from a patient

To show the localization of PR-WT and PR-B/L-mut protein in primary leukemia cells, IF staining using an anti-PML antibody was performed (Figure 7). Primary leukemia cells from patient 1 obtained at diagnosis and at the terminal stage were used to detect PR-WT and PR-B/L-mut, respectively. Nearly the same localization pattern as seen in Figure 5 was confirmed in this assay. The PML bodies were observed as a granular pattern at diagnosis (PR-WT), but the pattern was significantly altered to become diffuse at the terminal stage (PR-B/L-mut). These data strongly suggest that PR-B/L-mut protein was expressed and functional in primary leukemia cells, and may contribute to different responsiveness to As₂O₃ treatment.

Discussion

In the present study, we have shown acquired missense mutations in PML-RARA that are closely related to resistance to As₂O₃ treatment. In 2 patients, we detected A216V and L218P sub-

stitutions in the B2 domain of PML. The B2 domain is part of the RBCC motif, which is thought to be critical for PML homo-

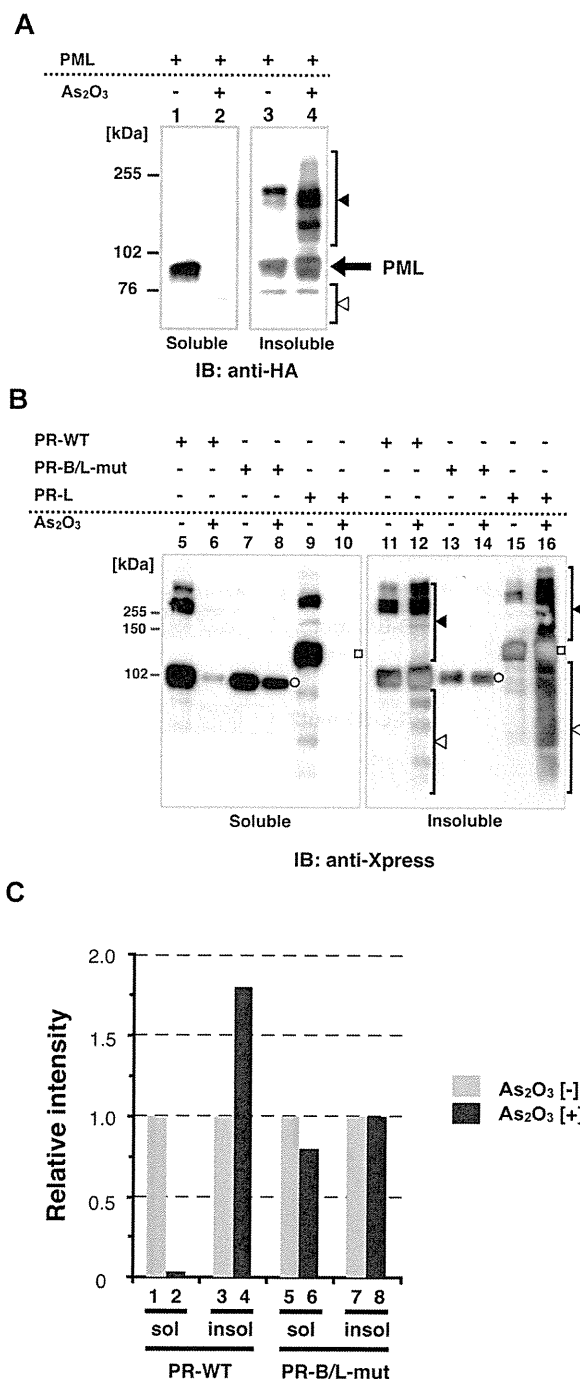


Figure 4. Protein localization of PML and its fusion proteins in soluble and/or insoluble fractions with or without As₂O₃. (A) HA-PML was overexpressed in HeLa cells with or without As₂O₃ (10 μM) for 2 hours, and the whole-cell lysate (soluble) and pellets (insoluble fraction) were obtained for immunoblotting. Black and white arrowheads indicate modified/oligomerized and degraded PML, respectively. (B) The same assay described in panel A was performed using PR-WT, PR-B/L-mut, and the long form of PML-RARA (PR-long). White circles indicate PR-WT or PR-B/L-mut and white squares indicate PR-long protein. Black and white arrowheads indicate modified/oligomerized and degraded fusion proteins, respectively. Note that neither protein transportation from the soluble to insoluble fraction (lanes 7 vs 8 and 13 vs 14) nor modified/oligomerized or degraded proteins after treatment with As₂O₃ (lanes 8 and 14) were observed with PR-B/L-mut. (C) Protein expression levels in panel B were measured using BioMax 1D software, and the relative intensity is depicted as a bar graph.

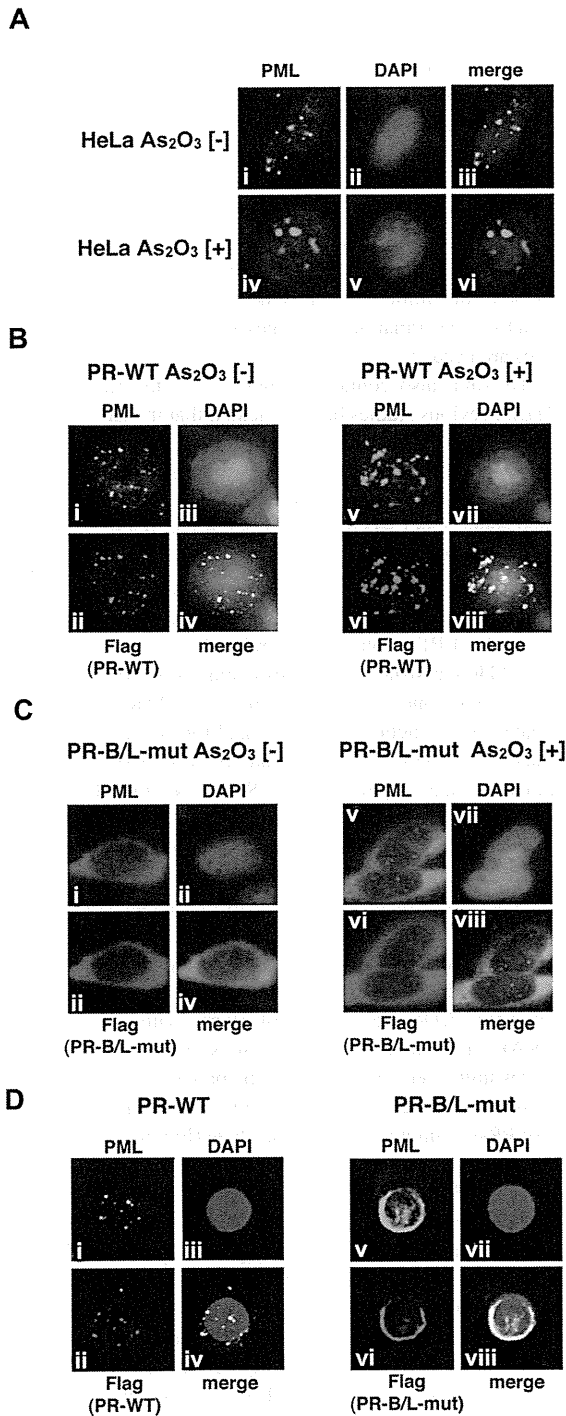


Figure 5. Analyses of the protein localization of PML, PR-WT, and PR-B/L-mut using IF staining. (A) HeLa cells were incubated with or without As₂O₃ (10 μM) for 8 hours, and endogenous PML was detected with an anti-PML antibody. PML nuclear bodies were detected in green. The nuclei were stained with 4,6 diamidino-2-phenylindole (DAPI; blue). Note that the microgranular pattern of NBs without As₂O₃ (i and iii) was altered to become a macrogranular pattern with As₂O₃ (iv and vi). (B) Flag-tagged PR-WT was used for the same assay as described in panel A. Anti-FLAG and anti-PML antibodies were used to detect PR-WT and endogenous PML, respectively. PML bodies were confirmed in the cytoplasm with a microgranular pattern without As₂O₃ (i, ii, and iv) and a macrogranular pattern with As₂O₃ (v, vi, and viii). (C) When using Flag-tagged PR-B/L-mut, localization showed a diffuse pattern mostly in the cytoplasm with and without As₂O₃. (D) Flag-tagged PR-WT or PR-B/L-mut was overexpressed in U937 cells without As₂O₃, and the same IF staining was performed. Note that PR-B/L-mut localization was confirmed in the cytoplasm as a diffuse pattern. Magnification is 800×.

heterodimerization, oligomerization, and As₂O₃ binding.^{23-25,34} Recent studies have indicated that As₂O₃ binds directly to cysteine residues in zinc fingers in the RBCC domain, especially C77/80 and C88/91 in the RING domain²⁴ and C212 and C213 in the B2 domain.²⁵ Binding of As₂O₃ in the RBCC domain appears to be critical for the effect of As₂O₃ on PML-RARA.^{24,25} Interestingly, the mutations described herein were located just adjacent to the CC motif (C212/213) in the B2 domain, which is thought to be critical for As₂O₃ binding (Figure 1D). These findings suggest that substitutions at A216 and L218 may affect proper As₂O₃ binding, resulting in aberrant responsiveness to As₂O₃ through aberrant subcellular localization, insufficient SUMOylation, and/or multimerization.

The in vitro SUMOylation assay indicated that PR-B/L-mut and PR-B2-mut mostly lack SUMO1-Ubc9-induced SUMOylation and dimerization/multimerization (Figure 3B), and this was not changed in the presence of As₂O₃. It has been suggested that degradation of the PML-RARA protein with As₂O₃, followed by SUMOylation and oligomerization,^{24,25} may also be inhibited by mutations in the B2 domain. Furthermore, PR-B/L-mut was localized in both the soluble and insoluble fractions, and the localization was not changed in the presence of As₂O₃. Nearly the same result was obtained with IF staining, indicating that PR-B/L-mut and PR-B2-mut were localized in the cytoplasm with a diffuse pattern that was not altered in the presence of As₂O₃ (Figure 5C). Furthermore, PR-L-B2-mut2 was localized in the nucleus as a diffuse pattern with or without As₂O₃ (Figure 6B). These results strongly suggest that amino acid substitution in the B2 domain is

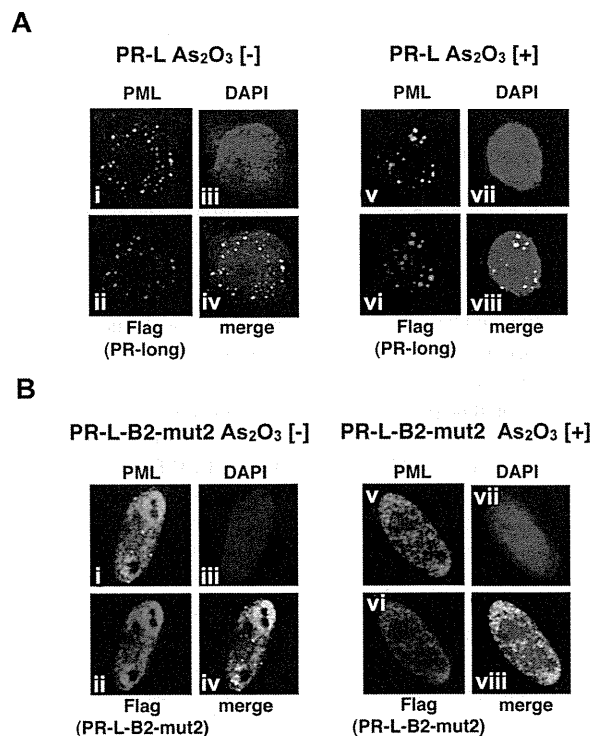


Figure 6. Analyses of the protein localization of PR-L and PR-L-B2-mut2 using IF staining. (A) Flag-tagged PR-L was overexpressed in HeLa cells with or without As₂O₃. Anti-FLAG and PML antibodies were used to detect PR-L and endogenous PML, respectively. PML bodies were confirmed in the nucleus with a microgranular pattern without As₂O₃ (i, ii, and iv) and a macrogranular pattern with As₂O₃ (v, vi, and viii). (B) A similar assay was performed using PR-L-B2-mut2. Note that the localization of PR-L-B2-mut2 was confirmed in the nucleus as a diffuse pattern with or without As₂O₃.

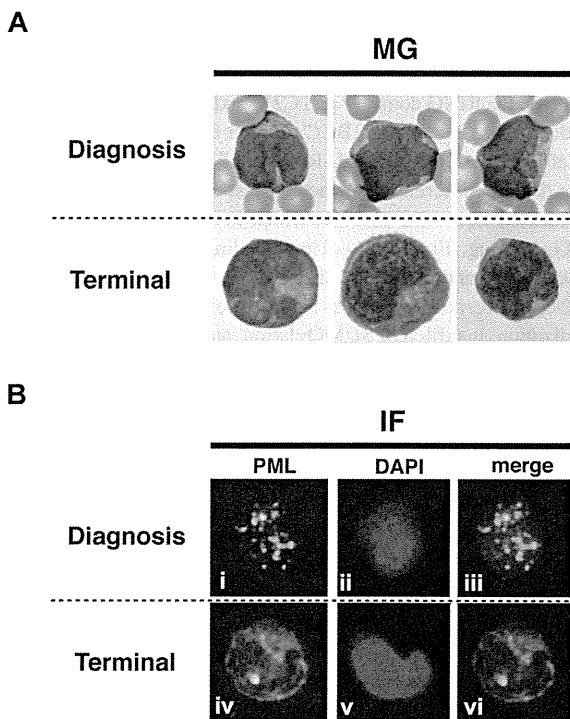


Figure 7. Protein localization of PML and its fusion proteins in primary leukemia cells from patient #1. May-Giemsa (MG) staining (A) and IF staining (B) are shown. The primary leukemia cells from patient 1 were obtained at diagnosis and at the terminal stage (shown as 1 and 5, respectively, in Figure 1A) and were used in this assay. PML nuclear bodies can be observed in the cells at diagnosis (i and iii), but at the terminal stage, PML and its fusion proteins were observed in the cytoplasm showing a diffuse pattern (iv and vi).

critical for the aberrant responsiveness *in vitro*, and the mutations may be critical for the resistance to As₂O₃ therapy *in vivo*.

In patient 6, only 2 of 20 clones (10%) contained a genetic mutation resulting in an L218P substitution in the B2 domain of the PML region. The genetic mutation was theoretically present in 20% of bone marrow cells, and the remaining 77% of leukemia cells (*PML-RARA*-positive cells [97.1%] in FISH analysis included *PML-RARA*-mutated cells [20%]) harbored wild-type *PML-RARA* according to the FISH analysis. Careful evaluation of whether the mutation contributes to clinical resistance to As₂O₃ therapy should be performed. Because clinically refractory disease against As₂O₃ was confirmed after the bone marrow aspiration, clonal expansion of *PML-RARA* with the L218P substitution may have been related to the insufficient responsiveness to As₂O₃ therapy. Another question is when the mutated clone appeared in this patient. One possibility is that the mutated clone was already present at the early stage of the disease. Genetic analysis using DNA obtained at the disease onset may be useful for clarifying this. Unfortunately, DNA obtained at the disease onset and the terminal stage of this patient was not available, and clarifying these issues is not currently possible. Further examination of additional patients and genetic analyses of samples obtained at several time points during the disease progression are required.

Interestingly, PR-B/L-mut was localized in the cytoplasm (Figures 5C and 6B), not in the nucleus. As reported previously, an NLS on the PML C-terminus is critical for transport into the nucleus.^{35,36} The absence of an NLS motif in the short form of *PML-RARA* (*bcr3*)^{32,37,38} may explain the cytoplasmic localization of PR-WT and PR-B/L-mut in our study. Furthermore, PR-B/L-

mut and -B2-mut showed a diffuse pattern (Figures 5C-D, 6B, and 7B). Borden et al³⁴ reported that substitution of conserved zinc finger domains in B1 and/or B2 disrupts PML nuclear body formation *in vivo*, and they also suggested that B1/B2 domains may be involved in the homo/hetero-oligomerization process via protein-protein interactions. Other studies have indicated that *PML-RARA* with mutations in B2 show a diffuse cytoplasmic pattern, perhaps because the mutated proteins cannot bind to nuclear body-forming proteins such as Daxx, Sp100, and SUMO-1, resulting in a failure to accumulate in the nuclear body.^{24,25,39,40} Amino acid substitution near the zinc finger motif in the B2 domain may lead to conformational changes in the PML protein. Further analyses are needed.

PR-B/L-mut also contains a mutation in the LBD of *RARA* (G391E). Previous studies have indicated that the LBD mutation is closely related to ATRA resistance,⁴¹⁻⁴⁴ and patient 1 in this study also showed a clinically refractory response to ATRA in the late stage of his disease progression and resistance to Am80 in the terminal stage. The LBD mutation G391E was detected only in the terminal stage (Figure 2B lanes 4 and 5). Therefore, an APL variant phenotype with *bcr3* of the *PML-RARA* protein may be related to a poor prognosis,^{32,37,38} showing that insufficient ATRA effectiveness and the LBD mutation are related to a consistent phenotype of ATRA resistance.⁴⁵ PR-B/L-mut is localized mainly in the cytoplasm, and the effectiveness of ATRA may not be anticipated. The function of PR-WT and PR-B/L-mut as transcription factors to control activation and/or repression by recruiting coregulators, such as p300/CBP, SMRT/N-CoR-TBL1/R1, and histone deacetylases,^{26,29,46,47} should be analyzed to confirm the responsiveness to ATRA. Conversely, the probability of the effects of the LBD mutation on As₂O₃ resistance may be relatively low based on our experiment, because the diffuse localization pattern in the cytoplasm of PR-B2-mut without an LBD mutation in the presence or absence of As₂O₃ showed nearly the same pattern as PR-B/L-mut (data not shown). Furthermore, a previous study indicated that ATRA-resistant NB4 clones with mutations in the *PML-RARA* LBD domain were fully sensitive to As₂O₃ treatment.⁴⁸

Interestingly, leukemia cells from patient 1 contained minor clones of PR-B2-mut and PR-LBD-mut in addition to the major clone of PR-B/L-mut at the terminal stage (Figure 2B time points 4 and 5), which is difficult to explain. One possibility is that one allele of the wild-type *PML* and *RARA* genes originally had genetic mutations in the B2 and LBD domains, and PR-WT, PR-B2-mut, PR-LBD-mut, and PR-B/L-mut were generated at the early stage of disease progression. Another explanation is that the *PML-RARA* fusion gene with mutations in the B2 and LBD domains translocated again with wild-type *PML* or *RARA* genes during the disease progression. Further analyses are required using several strategies including allele-specific PCR, FISH, and/or single nucleotide polymorphism analysis.

Mutations in the B2 domain that result in insufficient responsiveness to As₂O₃ therapy were confirmed in 2 of 15 (13%) patients with APL treated with As₂O₃. Recently, As₂O₃ was introduced as a consolidation treatment, and the event-free survival at 3 years was significantly improved compared with conventional consolidation treatment with ATRA and daunorubicin (80% vs 63%).¹² However, almost 5% of patients with APL treated with As₂O₃ show As₂O₃ refractory disease.⁴⁹ Because it is possible that a *PML* B2 mutation may be partly related to the As₂O₃ refractory phenotype, repeated genetic analyses at several time points of the clinical course may be useful for predicting patients at high risk for a poor

response to As₂O₃ therapy. Further investigation is required to confirm the clinical significance.

Acknowledgments

The authors thank Nobuhiko Emi, Kazuhito Yamamoto, Yukiyasu Ozawa, Taku Kimura, Keiko Niimi, Hiroshi Sao, Kazunori Ohnishi, and Hidehiko Saito for caring for the patients with APL and Tomoka Wakamatsu, Eriko Ushida, Manami Kira, Mari Otsuka, and Yukie Konishi for valuable laboratory assistance.

This work was supported by grants-in-aid for scientific research from the Ministry of Education, Culture, Sports, Science and Technology, Japan, and from the Public Trust Haraguchi Memorial Cancer Research Fund, Japan.

References

- Kakizuka A, Miller WH Jr, Umesono K, et al. Chromosomal translocation t(15;17) in human acute promyelocytic leukemia fuses RAR alpha with a novel putative transcription factor, PML. *Cell*. 1991;66(4):663-674.
- Huang ME, Ye YC, Chen SR, et al. Use of all-trans retinoic acid in the treatment of acute promyelocytic leukemia. *Blood*. 1988;72(2):567-572.
- Ohno R, Yoshida H, Fukutani H, et al. Multi-institutional study of all-trans-retinoic acid as a differentiation therapy of refractory acute promyelocytic leukemia. Leukaemia Study Group of the Ministry of Health and Welfare. *Leukemia*. 1993;7(11):1722-1727.
- Kanamaru A, Takemoto Y, Tanimoto M, et al. All-trans retinoic acid for the treatment of newly diagnosed acute promyelocytic leukemia. Japan Adult Leukemia Study Group. *Blood*. 1995;85(5):1202-1206.
- Lo-Coco F, Avvisati G, Vignetti M, et al. Front-line treatment of acute promyelocytic leukemia with AIDA induction followed by risk-adapted consolidation for adults younger than 61 years: results of the AIDA-2000 trial of the GIMEMA Group. *Blood*. 2010;116(17):3171-3179.
- Sanz MA, Montesinos P, Vellenga E, et al. Risk-adapted treatment of acute promyelocytic leukemia with all-trans retinoic acid and anthracycline monochemotherapy: long-term outcome of the LPA 99 multicenter study by the PETHEMA Group. *Blood*. 2008;112(8):3130-3134.
- Asou N, Kishimoto Y, Kiyoi H, et al. A randomized study with or without intensified maintenance chemotherapy in patients with acute promyelocytic leukemia who have become negative for PML-RARalpha transcript after consolidation therapy: the Japan Adult Leukemia Study Group (JALSG) APL97 study. *Blood*. 2007;110(1):59-66.
- Niu C, Yan H, Yu T, et al. Studies on treatment of acute promyelocytic leukemia with arsenic trioxide: remission induction, follow-up, and molecular monitoring in 11 newly diagnosed and 47 relapsed acute promyelocytic leukemia patients. *Blood*. 1999;94(10):3315-3324.
- Wang ZY, Chen Z. Acute promyelocytic leukemia: from highly fatal to highly curable. *Blood*. 2008;111(5):2505-2515.
- Shen ZX, Chen GQ, Ni JH, et al. Use of arsenic trioxide (As₂O₃) in the treatment of acute promyelocytic leukemia (APL): II. Clinical efficacy and pharmacokinetics in relapsed patients. *Blood*. 1997;89(9):3354-3360.
- Soignet SL, Frankel SR, Douer D, et al. United States multicenter study of arsenic trioxide in relapsed acute promyelocytic leukemia. *J Clin Oncol*. 2001;19(18):3852-3860.
- Powell BL, Moser B, Stock W, et al. Arsenic trioxide improves event-free and overall survival for adults with acute promyelocytic leukemia: North American Leukemia Intergroup Study C9710. *Blood*. 2010;116(19):3751-3757.
- Emadi A, Gore SD. Arsenic trioxide - An old drug rediscovered. *Blood Rev*. 2010;24(4-5):191-199.
- Zhu J, Koken MH, Quignon F, et al. Arsenic-induced PML targeting onto nuclear bodies: implications for the treatment of acute promyelocytic leukemia. *Proc Natl Acad Sci U S A*. 1997;94(8):3978-3983.
- Müller S, Matunis MJ, Dejean A. Conjugation with the ubiquitin-related modifier SUMO-1 regulates the partitioning of PML within the nucleus. *EMBO J*. 1998;17(1):61-70.
- Lallemand-Breitenbach V, Zhu J, Puvion F, et al. Role of promyelocytic leukemia (PML) sumolation in nuclear body formation, 11S proteasome recruitment, and As₂O₃-induced PML or PML/retinoic acid receptor alpha degradation. *J Exp Med*. 2001;193(12):1361-1371.
- Tatham MH, Geoffroy MC, Shen L, et al. RNF4 is a poly-SUMO-specific E3 ubiquitin ligase required for arsenic-induced PML degradation. *Nat Cell Biol*. 2008;10(5):538-546.
- Sun Y, Kim SH, Zhou DC, et al. Acute promyelocytic leukemia cell line AP-1060 established as a cytokine-dependent culture from a patient clinically resistant to all-trans retinoic acid and arsenic trioxide. *Leukemia*. 2004;18(7):1258-1269.
- Dai J, Weinberg RS, Waxman S, Jing Y. Malignant cells can be sensitized to undergo growth inhibition and apoptosis by arsenic trioxide through modulation of the glutathione redox system. *Blood*. 1999;93(1):268-277.
- Davison K, Cote S, Mader S, Miller WH. Glutathione depletion overcomes resistance to arsenic trioxide in arsenic-resistant cell lines. *Leukemia*. 2003;17(5):931-940.
- Kitamura K, Minami Y, Yamamoto K, et al. Involvement of CD95-independent caspase 8 activation in arsenic trioxide-induced apoptosis. *Leukemia*. 2000;14(10):1743-1750.
- Borden KL, Campbell Dwyer EJ, Salvato MS. An arenavirus RING (zinc-binding) protein binds the oncoprotein promyelocyte leukemia protein (PML) and relocates PML nuclear bodies to the cytoplasm. *J Virol*. 1998;72(1):758-766.
- Saurin AJ, Borden KL, Boddy MN, Freemont PS. Does this have a familiar RING? *Trends Biochem Sci*. 1996;21(6):208-214.
- Zhang XW, Yan XJ, Zhou ZR, et al. Arsenic trioxide controls the fate of the PML-RARalpha oncoprotein by directly binding PML. *Science*. 2010;328(5975):240-243.
- Jeanne M, Lallemand-Breitenbach V, Ferhi O, et al. PML/RAR oxidation and arsenic binding initiate the antileukemia response of As₂O₃. *Cancer Cell*. 2010;18(1):88-98.
- Atsumi A, Tomita A, Kiyoi H, Naoe T. Histone deacetylase 3 (HDAC3) is recruited to target promoters by PML-RARalpha as a component of the N-CoR co-repressor complex to repress transcription in vivo. *Biochem Biophys Res Commun*. 2006;345(4):1471-1480.
- Hiraga J, Tomita A, Sugimoto T, et al. Down-regulation of CD20 expression in B-cell lymphoma cells after treatment with rituximab-containing combination chemotherapies: its prevalence and clinical significance. *Blood*. 2009;113(20):4885-4893.
- Tomita A, Buchholz DR, Obata K, Shi YB. Fusion protein of retinoic acid receptor alpha with promyelocytic leukemia protein or promyelocytic leukemia zinc finger protein recruits N-CoR-TBLR1 corepressor complex to repress transcription in vivo. *J Biol Chem*. 2003;278(33):30788-30795.
- Tomita A, Buchholz DR, Shi YB. Recruitment of N-CoR/SMRT-TBLR1 corepressor complex by unliganded thyroid hormone receptor for gene repression during frog development. *Mol Cell Biol*. 2004;24(8):3337-3346.
- Hayakawa F, Privalsky ML. Phosphorylation of PML by mitogen-activated protein kinases plays a key role in arsenic trioxide-mediated apoptosis. *Cancer Cell*. 2004;5(4):389-401.
- Golomb HM, Rowley JD, Vardiman JW, Testa JR, Butler A. "Microgranular" acute promyelocytic leukemia: a distinct clinical, ultrastructural, and cytogenetic entity. *Blood*. 1980;55(2):253-259.
- Pandolfi PP, Alcalay M, Fagioli M, et al. Genomic variability and alternative splicing generate multiple PML/RAR alpha transcripts that encode aberrant PML proteins and PML/RAR alpha isoforms in acute promyelocytic leukaemia. *EMBO J*. 1992;11(4):1397-1407.
- Lallemand-Breitenbach V, Jeanne M, Benhenda S, et al. Arsenic degrades PML or PML-RARalpha through a SUMO-triggered RNF4/ubiquitin-mediated pathway. *Nat Cell Biol*. 2008;10(5):547-555.
- Borden KL, Lally JM, Martin SR, O'Reilly NJ, Solomon E, Freemont PS. In vivo and in vitro characterization of the B1 and B2 zinc-binding domains from the acute promyelocytic leukemia protooncoprotein PML. *Proc Natl Acad Sci U S A*. 1996;93(4):1601-1606.
- Flenghi L, Fagioli M, Tomassoni L, et al. Characterization of a new monoclonal antibody (PG-M3) directed against the aminoterminal portion of the PML gene product: immunocytochemical evidence for high expression of PML proteins on activated macrophages, endothelial cells, and epithelia. *Blood*. 1995;85(7):1871-1880.
- Fagioli M, Alcalay M, Tomassoni L, et al. Cooperation between the RING + B1-B2 and coiled-coil domains of PML is necessary for its effects

Authorship

Contribution: E.G., A.T., and F.H. designed the experiments, performed the research, and the analyzed data; E.G. and A.T. wrote the manuscript; A.A. prepared the clinical samples and performed the research; and A.T., H.K., and T.N. interpreted the data and supervised the experiments.

Conflict-of-interest disclosure: H.K. is a consultant for Kyowa Hakko Kogyo Co Ltd. The remaining authors declare no competing financial interests.

Correspondence: Akihiro Tomita, Department of Hematology and Oncology, Nagoya University Graduate School of Medicine, Tsurumai-cho 65, Showa-ku, Nagoya 466-8550, Japan; e-mail: atomita@med.nagoya-u.ac.jp.

- on cell survival. *Oncogene*. 1998;16(22):2905-2913.
37. Huang W, Sun GL, Li XS, et al. Acute promyelocytic leukemia: clinical relevance of two major PML-RAR alpha isoforms and detection of minimal residual disease by retrotranscriptase/polymerase chain reaction to predict relapse. *Blood*. 1993;82(4):1264-1269.
38. Vahdat L, Maslak P, Miller WH Jr, et al. Early mortality and the retinoic acid syndrome in acute promyelocytic leukemia: impact of leukocytosis, low-dose chemotherapy, PMN/RAR-alpha isoform, and CD13 expression in patients treated with all-trans retinoic acid. *Blood*. 1994;84(11):3843-3849.
39. Ishov AM, Sotnikov AG, Negorev D, et al. PML is critical for ND10 formation and recruits the PML-interacting protein daxx to this nuclear structure when modified by SUMO-1. *J Cell Biol*. 1999;147(2):221-234.
40. Lallemand-Breitenbach V, de Thé H. PML nuclear bodies. *Cold Spring Harb Perspect Biol*. 2010;2(5):a000661.
41. Zhou DC, Kim SH, Ding W, Schultz C, Warrell RP Jr, Gallagher RE. Frequent mutations in the ligand-binding domain of PML-RARalpha after multiple relapses of acute promyelocytic leukemia: analysis for functional relationship to response to all-trans retinoic acid and histone deacetylase inhibitors in vitro and in vivo. *Blood*. 2002;99(4):1356-1363.
42. Côté S, Zhou D, Bianchini A, Nervi C, Gallagher RE, Miller WH Jr. Altered ligand binding and transcriptional regulation by mutations in the PML/RARalpha ligand-binding domain arising in retinoic acid-resistant patients with acute promyelocytic leukemia. *Blood*. 2000;96(9):3200-3208.
43. Ding W, Li YP, Nobile LM, et al. Leukemic cellular retinoic acid resistance and missense mutations in the PML-RARalpha fusion gene after relapse of acute promyelocytic leukemia from treatment with all-trans retinoic acid and intensive chemotherapy. *Blood*. 1998;92(4):1172-1183.
44. Imaizumi M, Suzuki H, Yoshinari M, et al. Mutations in the E-domain of RAR portion of the PML/RAR chimeric gene may confer clinical resistance to all-trans retinoic acid in acute promyelocytic leukemia. *Blood*. 1998;92(2):374-382.
45. Marasca R, Zucchini P, Galimberti S, et al. Missense mutations in the PML/RARalpha ligand binding domain in ATRA-resistant As(2)O(3) sensitive relapsed acute promyelocytic leukemia. *Haematologica*. 1999;84(11):963-968.
46. Lin RJ, Nagy L, Inoue S, Shao W, Miller WH Jr, Evans RM. Role of the histone deacetylase complex in acute promyelocytic leukaemia. *Nature*. 1998;391(6669):811-814.
47. Grignani F, De Matteis S, Nervi C, et al. Fusion proteins of the retinoic acid receptor-alpha recruit histone deacetylase in promyelocytic leukaemia. *Nature*. 1998;391(6669):815-818.
48. Zhu Q, Zhang JW, Zhu HQ, et al. Synergic effects of arsenic trioxide and cAMP during acute promyelocytic leukemia cell maturation subtends a novel signaling cross-talk. *Blood*. 2002;99(3):1014-1022.
49. Zhou J, Zhang Y, Li J, et al. Single-agent arsenic trioxide in the treatment of children with newly diagnosed acute promyelocytic leukemia. *Blood*. 2010;115(9):1697-1702.

Extravascular hemolytic attack after eculizumab therapy for paroxysmal nocturnal hemoglobinuria

Akihiro Tomita · Yukari Shirasugi · Takahiko Ito · Hisashi Tsurumi · Tomoki Naoe

Received: 17 October 2011 / Accepted: 1 November 2011
© Springer-Verlag 2011

Dear Editor,

A 68-year-old man was diagnosed as having paroxysmal nocturnal hemoglobinuria (PNH) in 1998 and has had recurrent hyperchromic uria and anemia. Despite treatment with prednisone and cyclosporine, significant effectiveness was not observed in blood examination tests: hemoglobin (Hb), 5.0–10.0 g/dL; lactate dehydrogenase (LDH), 2,000–3,000 IU/L; and total bilirubin, 1.3–2.0 mg/dL. Red cell transfusions proceeded as required when hemolysis was severe. He was started on weekly 600 mg eculizumab (a humanized anti-C5 monoclonal antibody) for 4 doses in February 2008 and followed by biweekly 900 mg infusion. This resolved the hemoglobinuria, increased the Hb level, and decreased the LDH and bilirubin levels to almost normal ranges. Administration continued for 30 months.

After the administration of eculizumab on July 15, 2010, he had become soaked in heavy rainfall and developed a

chill. This was followed by a documented fever above 38°C for 4 days. On July 20, 2010, he was admitted to our hospital with symptoms of dyspnea on effort and icteric skin without documented fever. Blood tests revealed anemia (Hb 5.8 g/dL), elevated reticulocytes (107.8%), LDH (472 IU/L), and total bilirubin (6.6 mg/dL), as well as hyperurobilinogenuria without bilirubinuria and hemoglobinuria (Fig. 1). The direct antiglobulin test with anti-C3b and C3d antibodies was positive, whereas he had been negative before starting eculizumab in 2008. Supportive care with red blood cell transfusions and rehydration without steroid administration was performed, and blood examination tests mostly recovered within 4 weeks. These clinical features strongly suggest that extravascular hemolysis was closely related to the hemolytic attack after eculizumab administration.

Others have indicated that PNH red cells sometimes bind to C3 and show a CD55-negative/C3d-positive phenotype in flow cytometry after eculizumab therapy, when such cells might correlate somewhat with “chronic” hemolytic anemia [1–5]. The inflammatory condition induced in our patient by infection preceding the documented fever might have been related to the rapid activation of opsonized PNH red cell binding to C3 by macrophages in the extravascular space of the spleen and/or liver. Laboratory data differed between intravascular and extravascular hemolytic attack in this patient (Table 1). A relatively low LDH (<1,000 IU) and high bilirubin levels compared with the severity of hemolytic anemia, hyperurobilinogenuria without hemoglobin and hemosiderinuria, and a positive direct antiglobulin test might indicate extravascular hemolytic attack. Low haptoglobin levels in this patient were not a good indicator of extravascular hemolytic attack, because the values were below the lower limit even when his condition was stabilized during eculizumab therapy. Analysis by FCM using anti-C3b/d antibody for PNH red cells while in stable

A. Tomita (✉) · T. Naoe
Department of Hematology and Oncology,
Nagoya University Graduate School of Medicine,
Tsurumai-cho 65, Showa-ku,
Nagoya 466-8550, Japan
e-mail: atomita@med.nagoya-u.ac.jp

Y. Shirasugi
Department of Hematology and Oncology,
Tokai University Hospital,
Isehara, Japan

T. Ito
Department of Hematology, Gifu Social Insurance Hospital,
Kani, Japan

H. Tsurumi
First Department of Internal Medicine,
Gifu University Graduate School of Medicine,
Gifu, Japan

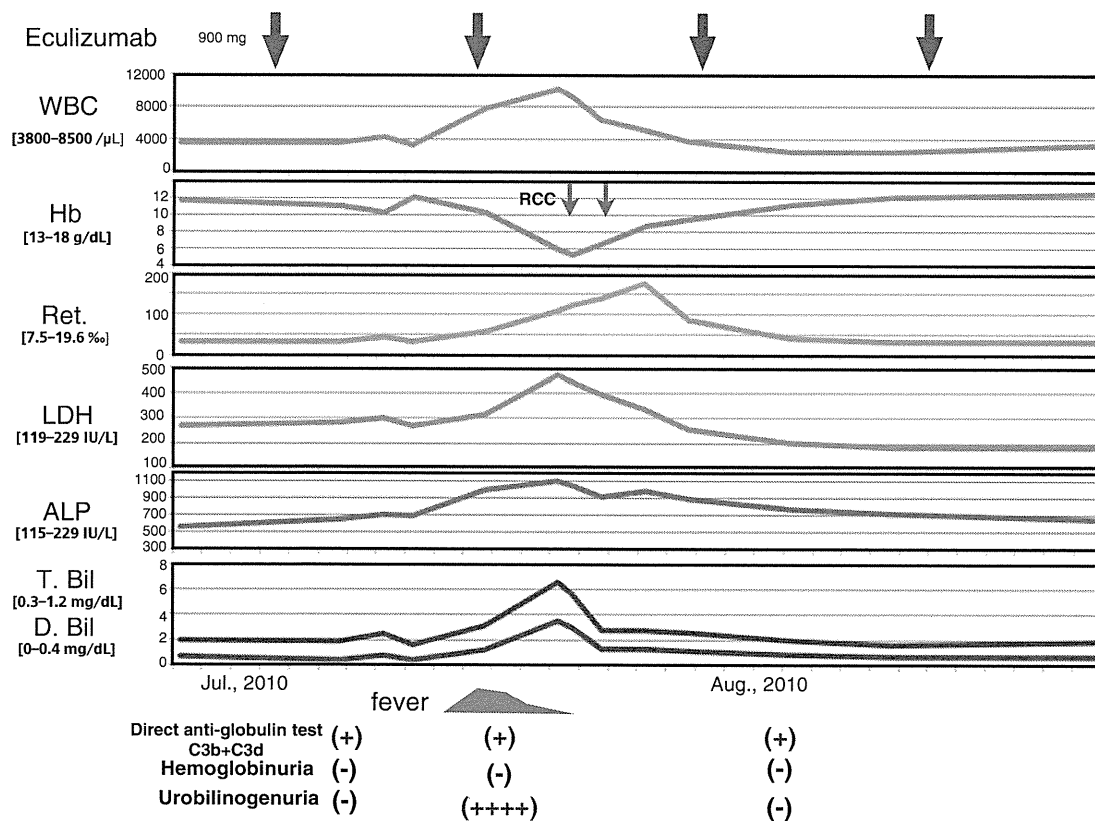


Fig. 1 Clinical course of extravascular hemolytic attack after eculizumab administration in a patient with PNH. Eculizumab (900 mg) was administered biweekly for 30 months. Hemolytic attack was confirmed after documented fever. White blood cell count (*WBC*), LDH, reticulocytes (*Ret.*), alkaline phosphatase (*ALP*), and bilirubin (total and direct bilirubin; *T. Bil* and *D. Bil*) were transiently elevated

after the fever. Hemoglobin and hemosiderinuria did not occur during this event although significant urobilinogenuria was confirmed. Direct antiglobulin test findings using anti-C3b and anti-C3d antibodies were positive during this event. *RCC* red blood cell transfusion. The normal range of the laboratory data are indicated in *square brackets*

condition might be helpful for quantifying the number of PNH red cells that bind to C3 and for predicting extravascular hemolytic attack. Notably, eculizumab remained effective in preventing intravascular hemolysis

by blocking C5 function throughout this period. Continued eculizumab administration is recommended even during extravascular hemolytic attack to prevent the intravascular hemolysis of PNH red cells.

Table 1 Laboratory data of the PNH patient at intravascular and extravascular hemolytic attack

Clinical data	Intravascular hemolysis before eculizumab	Extravascular hemolysis after eculizumab
Hemoglobinuria	+++	-
Urobilinogenuria	+-	++++
Bilirubinuria	-	-
WBC elevation (μL)	-	+ (10,000–11,000)
LDH elevation (IU/L)	+++ (2,000–3,000)	+ (400–500)
Bilirubin elevation (mg/dL)	+ (1.4–2.0)	++ (6.0–7.0)
AST elevation (IU/L)	++ (100–140)	-~+ (40–50)
CRP elevation	-	++
Haptoglobin decrease	+	+
Direct antiglobulin test (C3b+C3d)	-	+
Symptom of infection	-	+

Conflict of interest/disclosure All authors declare no competing financial interests.

References

1. Luzzatto L, Gianfaldoni G, Notaro R (2011) Management of paroxysmal nocturnal haemoglobinuria: a personal view. *Br J Haematol* 153(6):709–720
2. Berzuini A, Montanelli F, Prati D (2010) Hemolytic anemia after eculizumab in paroxysmal nocturnal hemoglobinuria. *N Engl J Med* 363(10):993–994
3. Hill A, Rother RP, Wang X, Morris SM Jr, Quinn-Senger K, Kelly R, Richards SJ, Bessler M, Bell L, Hillmen P, Gladwin MT (2010) Effect of eculizumab on haemolysis-associated nitric oxide depletion, dyspnoea, and measures of pulmonary hypertension in patients with paroxysmal nocturnal haemoglobinuria. *Br J Haematol* 149(3):414–425
4. Risitano AM, Notaro R, Luzzatto L, Hill A, Kelly R, Hillmen P (2010) Paroxysmal nocturnal hemoglobinuria–hemolysis before and after eculizumab. *N Engl J Med* 363(23):2270–2272
5. Risitano AM, Notaro R, Marando L, Serio B, Ranaldi D, Seneca E, Ricci P, Alfinito F, Camera A, Gianfaldoni G, Amendola A, Boschetti C, Di Bona E, Fratellanza G, Barbano F, Rodeghiero F, Zanella A, Iori AP, Selleri C, Luzzatto L, Rotoli B (2009) Complement fraction 3 binding on erythrocytes as additional mechanism of disease in paroxysmal nocturnal hemoglobinuria patients treated by eculizumab. *Blood* 113(17):4094–4100

An Epstein-Barr Virus-Associated Leukemic Lymphoma in a Patient Treated with Rabbit Antithymocyte Globulin and Cyclosporine for Hepatitis-Associated Aplastic Anemia

Kinya Ohata Noriko Iwaki Takeharu Kotani Yukio Kondo Hirohito Yamazaki
Shinji Nakao

Cellular Transplantation Biology, Kanazawa University Graduate School of Medical Science, Kanazawa, Japan

Key Words

Antithymocyte globulin · Aplastic anemia · Diffuse large B-cell lymphoma · Epstein-Barr virus · Lymphoproliferative disorder

Abstract

Lymphoproliferative disorders (LPDs) are generally caused by uncontrolled B-cell proliferation induced by the Epstein-Barr virus (EBV) in the setting of impaired EBV-specific T-cell immunity, particularly when there is pharmacological immunosuppression including antithymocyte globulin. We herein present an unusual case of EBV associated with LPD (EBV-LPD) in which LPD occurred 3 weeks after the use of rabbit antithymocyte globulin administered for severe hepatitis-associated aplastic anemia; the patient died of fulminant leukemic lymphoma 5 days after the onset. We also review the pertinent literature on EBV-LPD after immunosuppressive therapy and document the efficacy of EBV viral load monitoring and the need for preemptive therapy.

Copyright © 2011 S. Karger AG, Basel

Introduction

Epstein-Barr virus (EBV)-associated lymphoproliferative disorders (LPDs) are becoming a serious problem with a recent increase in the number of patients with immunodeficiency. In particular, patients who have undergone allogeneic hematopoietic stem cell transplantation (HSCT) are predisposed to EBV infection or reactivation and development of EBV-related diseases [1]. EBV monitoring is generally recommended for high-risk patients such as HSCT recipients of human leukocyte antigen mismatched donors and patients receiving antithymocyte globulin (ATG) after HSCT. Early detection of EBV reactivation would make it possible to offer preemptive therapy with rituximab if necessary, thus preventing the proliferation of EBV-infected B cells and the evolution of B-cell lymphoma.

Acquired severe aplastic anemia (SAA) is a rare disease defined by peripheral blood pancytopenia associated with hypocellularity of the bone marrow [2]. Because bone marrow failure is thought to result from an immune-mediated mechanism, immunosuppressive therapy (IST) is the treatment of choice in patients without a suitable donor for HSCT. IST including ATG and cyclosporine A (CsA) is the most effective treatment for SAA [3]. Several studies have shown that the use of ATG increases the fre-

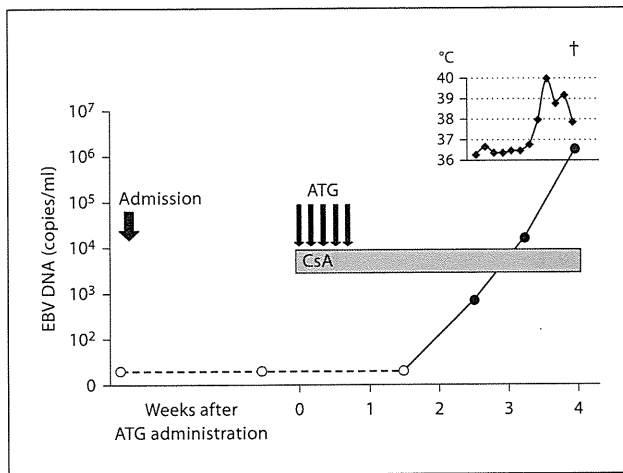


Fig. 1. Changes in plasma EBV DNA and the patient's body temperature. Open and closed circles represent EBV-negative and -positive states, respectively. Increase in EBV DNA was observed 2 weeks after administration of ATG.

quency of EBV reactivation and the risk of EBV-LPD [4]. However, this risk has not yet been sufficiently documented in patients treated with ATG for SAA. It is also unclear whether EBV viral load monitoring during IST for SAA and subsequent preemptive therapy are beneficial [5, 6].

We herein report an unusual case of fulminant EBV-LPD that occurred in a patient as a form of leukemic lymphoma 3 weeks after the first administration of rabbit ATG and CsA for hepatitis-associated AA.

Case Report

A 54-year-old male presented to the hospital with a 3-week history of general malaise and loss of appetite. He showed jaundice and had severely deranged liver function tests, with a total bilirubin of 5.5 mg/dl (normal range 0.3–1.2, direct fraction 3.1), alkaline phosphatase 536 IU/l (normal range 115–359), aspartate aminotransferase 1,021 IU/l (normal range 13–33), alanine aminotransferase 2,718 IU/l (normal range 8–42) and γ -glutamyl transpeptidase 288 IU/l (normal range 10–47). His blood tests showed a platelet count of $12 \times 10^9/l$, a hemoglobin level of 13.1 g/dl and a white blood cell (WBC) count of $1.4 \times 10^9/l$, with $0.7 \times 10^9/l$ neutrophils. The absolute counts of CD4- and CD8-positive T cells were 0.2 and $0.1 \times 10^9/l$, respectively. A blood film showed leukopenia and thrombocytopenia, with no abnormal morphology. There was no history of recent travel, blood transfusions, use of medications or excess alcohol consumption. Subsequent investigations showed no evidence of a viral etiology. Hepatitis A virus immunoglobulin M (IgM), hepatitis B virus antigen, hepatitis B core IgM, hepatitis C virus antibody, hepatitis C RNA

PCR, hepatitis E virus IgM and IgG were all negative. The hepatitis B surface antibody was positive, but hepatitis B virus PCR was negative. The cytomegalovirus IgG was positive and cytomegalovirus IgM was weakly positive. His anti-EBV antibody titers were viral capsid antigen IgG positive, viral capsid antigen IgM negative, early antigen negative, and EBV-determined nuclear antigen positive. Parvovirus B19 IgM and IgG serology were negative. The patient was also negative for HIV antibodies. The bone marrow was severely hypocellular, which was consistent with AA. Immunophenotyping of bone marrow cells was normal, and there was no evidence of paroxysmal nocturnal hemoglobinuria. A liver biopsy was not performed due to the presence of severe thrombocytopenia. We diagnosed him with hepatitis-associated AA. ATG therapy was put on hold until his liver function tests improved, but his pancytopenia progressed without normalization of his jaundice. Rabbit ATG was started 3 weeks after admission at a dose of 3.75 mg/kg on days 1–5, and CsA at a dose of 3 mg/kg with methylprednisolone, which resulted in a rapid improvement in his liver function. He was further treated with prednisolone for prophylaxis of serum sickness, with normalization of liver function tests, but his hematological data still showed pancytopenia.

Three weeks after the administration of ATG, the patient developed a persistent high fever, which was refractory to antibiotics and antifungal agents. Moreover, his liver function tests worsened, including a total bilirubin of 1.9 mg/dl, aspartate aminotransferase 408 IU/l, alanine aminotransferase 577 IU/l, γ -glutamyl transpeptidase 779 IU/l, and alkaline phosphatase 848 IU/l. Blood tests showed a platelet count of $15 \times 10^9/l$, a hemoglobin level of 9.2 g/dl and a WBC count of $7.5 \times 10^9/l$. A peripheral blood smear revealed an increased number of lymphocytes ($2.0 \times 10^9/l$), but no apparent hemophagocytic findings. The phenotype of the atypical lymphocytes was CD3-, CD10-, CD19+, CD20+ and IgG light chain lambda+. The serum ferritin level (199,770 ng/ml) was also markedly elevated. Based on these clinical signs, laboratory data and the use of ATG, EBV-LPD was highly suspected. The administration of rituximab was considered, but severe metabolic acidosis and cardiorespiratory failure developed the evening after EBV-LPD was diagnosed and the patient died of LPD on the following day.

The related results of the peripheral blood EBV DNA (3.3×10^6 copies/ 10^6 WBC) and the pathological examination from the liver biopsy (demonstrating an increase in CD20+ lymphocytes that were positive for EBV-encoded mRNA by in situ hybridization) confirmed the diagnosis of EBV-associated diffuse large B-cell lymphoma. Infiltration of the lymphoma was also detected in his bone marrow. We analyzed the patient's peripheral plasma EBV DNA retrospectively. His plasma showed an elevation of the EBV viral load to 700 copies/ml for the first time at 7 days before the onset of pyrexia, and the EBV viral load rapidly increased within 5 days (fig. 1).

Discussion

We herein describe the occurrence of fulminant EBV-LPD that was diagnosed following a sharp increase in the atypical B-cell count in peripheral blood 3 weeks after IST for hepatitis-associated AA. The patient died of car-

Table 1. Reports of LPD after IST for AA

References	Age, years	sex	Type of LPD	Immunosuppression
Dorr et al. [8], 1996	17	female	lymphoma	ATG, CsA
Saranghi et al. [9], 1999	22	male	T-ALL	CsA
Takeuchi et al. [10], 2000	54	female	B-ALL	CsA, PSL=, others
Hirose et al. [11], 2001	24	male	T-ALL	CsA
Calistri et al. [12], 2006	38	male	infectious mononucleosis	rATG, CsA, M-PSL → hATG
Wondergem et al. [6], 2008	42	female	EBV(+) DLBCL	hATG, CsA → rATG, CsA
Suzuki et al. [13], 2009	63	female	EBV(-) DLBCL	ATG, CsA
Viola et al. [14], 2011	55	male	EBV(+) plasma cell hyperplasia	hATG
Our case	54	male	EBV(+) DLBCL	rATG, CsA, PSL

T-ALL = T-cell acute lymphoblastic leukemia; B-ALL = B-cell acute lymphoblastic leukemia; PSL = prednisolone; rATG = rabbit ATG; M-PSL = methylprednisolone; hATG = horse ATG; DLBCL = diffuse large B-cell lymphoma.

diorespiratory failure associated with severe lactic acidosis due to rapidly progressive lymphoma. Lactic acidosis in association with hematologic malignancies normally shows an extremely poor prognosis [7].

It is well documented that EBV is an important complication of prolonged immunodeficiency. All patients who have a limited number of circulating T cells and retain B cells are at risk of developing EBV reactivation, as the interplay among EBV replication, latency and immune control is not as balanced as in the healthy host. When there is pharmacological immunosuppression, EBV reactivation can lead to LPD because T-cell function is severely impaired and B cells can evade the T-cell attack and expand. This is particularly common in patients undergoing HSCT with an ATG-containing conditioning regimen [4].

Treatment with ATG combined with CsA is the standard therapeutic approach to SAA. Scheinberg et al. [5] showed the risk of EBV disease in patients treated with ATG for AA to be low. In their study of 78 patients with SAA who had received 4 different immunosuppressive regimens, including ATG, even though EBV reactivation occurred in most patients, none developed symptomatic EBV-LPD. To determine the incidence of clinically significant EBV-LPD, we searched Medline for published articles about LPD after IST for AA. As shown in table 1, a total of 8 cases of LPD that occurred after IST have been reported [6, 8–14].

Viola et al. [14] recently reported a patient who developed LPD 1 month after the use of horse ATG for the treatment of SAA. Although the interval between ATG therapy and the onset of LPD in this case was short, similar to our case, he had received chemotherapy and au-

tologous HSCT for the treatment of non-Hodgkin's lymphoma 3 years prior to the ATG therapy, both of which may have predisposed the patient to develop LPD.

Wondergem et al. [6] described a patient who received a higher dose of rabbit ATG for SAA after failing to respond to horse ATG. The patient then developed life-threatening EBV-related lymphoma. In our patient, LPD occurred after his first ATG therapy. To the best of our knowledge, this is the first report of an EBV-related diffuse large B-cell lymphoma in a patient treated with a single course of rabbit ATG.

Recently, the viral load has been shown to be a significant predictor of EBV-related post-transplant LPD [15, 16], and early treatment with an anti-CD20 antibody is recommended as preemptive therapy in patients undergoing an alternative donor transplant [1]. Because of the rapid clinical course of EBV-LPD, immediate treatment is crucial to reduce mortality [6]. No lymphocytosis or pyrexia was observed when the EBV DNA level began to increase in our patient (fig. 1). Preemptive therapy with rituximab may improve the treatment outcome of EBV-LPD, not only after HSCT [17], but also after IST for SAA. However, the EBV copy number in the plasma of the current patient at day 19 of ATG therapy, 1 week before the onset of pyrexia, was 700 copies/ml, but it increased by more than 20 fold on day 24 (16,000 copies/ml). Therefore, once-a-week screening of EBV would have been useless for this patient. The prompt examination of blood for EBV copy number in response to clinical signs such as pyrexia may be more practical than surveillance for appropriately starting rituximab. The preventive administration of rituximab would be a possible option for AA patients with a high risk of developing EBV-LPD.

Several risk factors for susceptibility to EBV-related lymphoma have been identified. Dierksheide et al. [18] showed that an interferon- γ polymorphism affects a likelihood of EBV reactivation. Genotyping of the interferon- γ gene may be useful for identifying patients at greater risk of developing EBV-LPD. The percentage of CD4+ T cells in hepatitis-associated AA patients is reported to be significantly lower than that in non-hepatitis-associated AA patients [19]. Therefore, the presence of hepatitis-associated AA may have predisposed our patient to developing EBV-LPD.

The short time interval between ATG treatment and diagnosis and the fulminant course of EBV-LPD in our case and in the case reported by Viola et al. [14] may be related to the profound immunosuppressive state associated with hepatitis and the precedent chemotherapy in these cases.

The present case indicates that fulminant EBV-associated lymphoma can occur in patients with AA even after a single course of rabbit ATG therapy. Close monitoring of the EBV viral load is therefore a prerequisite for rabbit ATG therapy of AA.

References

- van Esser JW, van der Holt B, Meijer E, Niesters HG, Trenschele R, Thijsen SF, van Loon AM, Frassoni F, Bacigalupo A, Schaefer UW, Osterhaus AD, Gratama JW, Lowenberg B, Verdonck LF, Cornelissen JJ: Epstein-Barr virus (EBV) reactivation is a frequent event after allogeneic stem cell transplantation (SCT) and quantitatively predicts EBV-lymphoproliferative disease following T-cell-depleted SCT. *Blood* 2001;98:972-978.
- Young NS, Calado RT, Scheinberg P: Current concepts in the pathophysiology and treatment of aplastic anemia. *Blood* 2006;108:2509-2519.
- Teramura M, Kimura A, Iwase S, Yonemura Y, Nakao S, Urabe A, Omine M, Mizoguchi H: Treatment of severe aplastic anemia with antithymocyte globulin and cyclosporin A with or without G-CSF in adults: a multicenter randomized study in Japan. *Blood* 2007;110:1756-1761.
- Bacigalupo A: Antilymphocyte/thymocyte globulin for graft versus host disease prophylaxis: efficacy and side effects. *Bone Marrow Transplant* 2005;35:225-231.
- Scheinberg P, Fischer SH, Li L, Nunez O, Wu CO, Sloand EM, Cohen JI, Young NS, John Barrett A: Distinct EBV and CMV reactivation patterns following antibody-based immunosuppressive regimens in patients with severe aplastic anemia. *Blood* 2007;109:3219-3224.
- Wundergem MJ, Stevens SJ, Janssen JJ, Oudejans JJ, Ossenkoppele GJ, Middeldorp JM, Zweegman S: Monitoring of EBV reactivation is justified in patients with aplastic anemia treated with rabbit ATG as a second course of immunosuppression. *Blood* 2008;111:1739, author reply 1739-1740.
- Sillos EM, Shenep JL, Burghen GA, Pui CH, Behm FG, Sandlund JT: Lactic acidosis: a metabolic complication of hematologic malignancies: case report and review of the literature. *Cancer* 2001;92:2237-2246.
- Dorr V, Doolittle G, Woodroof J: First report of a B cell lymphoproliferative disorder arising in a patient treated with immune suppressants for severe aplastic anemia. *Am J Hematol* 1996;52:108-113.
- Sarangi JN, Kashyap R, Choudhry VP, Mishra DK, Saxena R, Gurbaxani S, Bhargava M: Severe aplastic anemia evolving into T cell acute lymphoblastic leukemia. *Eur J Haematol* 1999;63:269-271.
- Takeuchi M, Soda R, Takahashi K, Kimura F, Lai M, Ueda Y: Philadelphia chromosome positive acute lymphocytic leukemia arising from aplastic anemia. *Am J Hematol* 2000;63:161-162.
- Hirose Y, Masaki Y, Ebata K, Okada J, Kim CG, Ogawa N, Wano Y, Sugai S: T-cell type acute lymphoblastic leukemia following cyclosporin A therapy for aplastic anemia. *Int J Hematol* 2001;73:226-229.
- Calistri E, Tiribelli M, Battista M, Michelutti A, Corbellino M, Viale P, Fanin R, Damiani D: Epstein-Barr virus reactivation in a patient treated with anti-thymocyte globulin for severe aplastic anemia. *Am J Hematol* 2006;81:355-357.
- Suzuki Y, Niitsu N, Hayama M, Katayama T, Ishii R, Osaka M, Miyazaki K, Danbara M, Horie R, Yoshida T, Nakamura N, Higashihara M: Lymphoproliferative disorders after immunosuppressive therapy for aplastic anemia: a case report and literature review. *Acta Haematol* 2009;121:21-26.
- Viola GM, Zu Y, Baker KR, Aslam S: Epstein-Barr virus-related lymphoproliferative disorder induced by equine anti-thymocyte globulin therapy. *Med Oncol* 2011;28:1604-1608.
- Aalto SM, Juvonen E, Tarkkanen J, Volin L, Haario H, Ruutu T, Hedman K: Epstein-Barr viral load and disease prediction in a large cohort of allogeneic stem cell transplant recipients. *Clin Infect Dis* 2007;45:1305-1309.
- Wagner HJ, Cheng YC, Huls MH, Gee AP, Kuehnle I, Krance RA, Brenner MK, Rooney CM, Heslop HE: Prompt versus preemptive intervention for EBV lymphoproliferative disease. *Blood* 2004;103:3979-3981.
- van Esser JW, Niesters HG, van der Holt B, Meijer E, Osterhaus AD, Gratama JW, Verdonck LF, Lowenberg B, Cornelissen JJ: Prevention of Epstein-Barr virus-lymphoproliferative disease by molecular monitoring and preemptive rituximab in high-risk patients after allogeneic stem cell transplantation. *Blood* 2002;99:4364-4369.
- Dierksheide JE, Baiocchi RA, Ferketich AK, Roychowdhury S, Pelletier RP, Eisenbeis CF, Caligiuri MA, VanBuskirk AM: IFN-gamma gene polymorphisms associate with development of EBV+ lymphoproliferative disease in hu PBL-SCID mice. *Blood* 2005;105:1558-1565.
- Kojima S, Matsuyama K, Koderia Y, Okada J: Circulating activated suppressor T lymphocytes in hepatitis-associated aplastic anaemia. *Br J Haematol* 1989;71:147-151.

blood

2011 118: 6601-6609
Prepublished online September 30, 2011;
doi:10.1182/blood-2011-07-365189

Frequent loss of HLA alleles associated with copy number-neutral 6pLOH in acquired aplastic anemia

Takamasa Katagiri, Aiko Sato-Otsubo, Koichi Kashiwase, Satoko Morishima, Yusuke Sato, Yuka Mori, Motohiro Kato, Masashi Sanada, Yasuo Morishima, Kohei Hosokawa, Yumi Sasaki, Shigeki Ohtake, Seishi Ogawa, Shinji Nakao and on behalf of the Japan Marrow Donor Program

Updated information and services can be found at:
<http://bloodjournal.hematologylibrary.org/content/118/25/6601.full.html>

Articles on similar topics can be found in the following Blood collections
Hematopoiesis and Stem Cells (2967 articles)
Immunobiology (4699 articles)

Information about reproducing this article in parts or in its entirety may be found online at:
http://bloodjournal.hematologylibrary.org/site/misc/rights.xhtml#repub_requests

Information about ordering reprints may be found online at:
<http://bloodjournal.hematologylibrary.org/site/misc/rights.xhtml#reprints>

Information about subscriptions and ASH membership may be found online at:
<http://bloodjournal.hematologylibrary.org/site/subscriptions/index.xhtml>

Blood (print ISSN 0006-4971, online ISSN 1528-0020), is published weekly by the American Society of Hematology, 2021 L St, NW, Suite 900, Washington DC 20036.
Copyright 2011 by The American Society of Hematology; all rights reserved.



Frequent loss of HLA alleles associated with copy number-neutral 6pLOH in acquired aplastic anemia

*Takamasa Katagiri,^{1,2} *Aiko Sato-Otsubo,³ Koichi Kashiwase,^{4,5} Satoko Morishima,⁶ Yusuke Sato,³ Yuka Mori,³ Motohiro Kato,³ Masashi Sanada,³ Yasuo Morishima,⁷ Kohei Hosokawa,² Yumi Sasaki,² Shigeki Ohtake,¹ †Seishi Ogawa,^{3,5} and †Shinji Nakao,² on behalf of the Japan Marrow Donor Program

¹Clinical Laboratory Science, Division of Health Sciences, and ²Cellular Transplantation Biology, Kanazawa University Graduate School of Medical Science, Ishikawa, Japan; ³Cancer Genomics Project, Graduate School of Medicine, University of Tokyo, Tokyo, Japan; ⁴Tokyo Metropolitan Red Cross Blood Center, Tokyo, Japan; ⁵Core Research for Evolutional Science and Technology, Exploratory Research for Advanced Technology, Japan Science and Technology Agency, Saitama, Japan; ⁶Department of Hematology, Fujita Health University, Aichi, Japan; and ⁷Department of Hematology and Cell Therapy, Aichi Cancer Center Hospital, Nagoya, Japan

Idiopathic aplastic anemia (AA) is a common cause of acquired BM failure. Although autoimmunity to hematopoietic progenitors is thought to be responsible for its pathogenesis, little is known about the molecular basis of this autoimmunity. Here we show that a substantial proportion of AA patients harbor clonal hematopoiesis characterized by the presence of acquired copy number-neutral loss of heterozygosity (CNN-LOH) of the 6p arms (6pLOH). The 6pLOH commonly involved

the HLA locus, leading to loss of one HLA haplotype. Loss of HLA-A expression from multiple lineages of leukocytes was confirmed by flow cytometry in all 6pLOH(+) cases. Surprisingly, the missing HLA-alleles in 6pLOH(+) clones were conspicuously biased to particular alleles, including HLA-A*02:01, A*02:06, A*31:01, and B*40:02. A large-scale epidemiologic study on the HLA alleles of patients with various hematologic diseases revealed that the 4 HLA alleles were over-represented

in the germline of AA patients. These findings indicate that the 6pLOH(+) hematopoiesis found in AA represents “escapes” hematopoiesis from the autoimmunity, which is mediated by cytotoxic T cells that target the relevant autoantigens presented on hematopoietic progenitors through these class I HLAs. Our results provide a novel insight into the genetic basis of the pathogenesis of AA. (*Blood*. 2011;118(25):6601-6609)

Introduction

Acquired aplastic anemia (AA) is a rare condition associated with BM failure and pancytopenia.¹ A series of classic observations and experiments have unequivocally supported that the autoimmunity to hematopoietic stem/progenitor cells (HSPCs) critically underlies the pathogenesis of the BM failure in the majority of AA cases. According to the widely accepted model of immune-mediated BM failure, activated cytotoxic T cells (CTLs) that recognize an auto-antigen(s) presented on HSPCs through their class I HLA molecules have a major role in initiating the autoimmune reactions.²⁻⁴ However, no definitive evidence exists that supports this model or the presence of such CTL repertoires. Moreover, little information is available about their target antigens or about the way by which they are recognized by effector T cells.

Another long-standing issue on AA is its close relationship with clonal hematopoiesis.^{5,6} It was first suspected from an apparent overlap between AA and paroxysmal nocturnal hemoglobinuria (PNH)^{7,8} and was also implicated by the frequent development of late clonal disorders in AA, such as myelodysplastic syndromes, PNH, or even acute myeloid leukemia (AML).⁹⁻¹¹ Clonal hematopoiesis can be explicitly demonstrated by conventional clonality assays at presentation in a substantial proportion of newly diagnosed typical AA cases.¹² Although it has been expected that the inciting autoimmune insult somehow confers selective pressures on the evolution of clonal hematopoiesis,⁵ the exact mechanism for such immunologic selection or escape is still unclear.

The objectives of this study, therefore, were to characterize the clonal nature of the hematopoiesis that is maintained even under the severe autoimmune insult in AA, and to explore the genetic/immunologic mechanism that could underlie the pathogenesis of AA. To achieve these aims, we performed single nucleotide polymorphism (SNP) array-based analysis of genomic copy numbers and/or allelic imbalances in peripheral blood (PB) specimens obtained from 306 patients with AA. Initially, we found that AA patients frequently showed clonal/oligoclonal hematopoiesis that lost specific HLA alleles as a result of copy number-neutral loss of heterozygosity (CNN-LOH) of the 6p arms, which led us to further analyses of the contribution of 6pLOH(+) clones to residual hematopoiesis and a large-scale epidemiologic study on the HLA alleles that are over-represented in AA, involving a total of 6,613 transplants registered in the Japan Marrow Donor Program (JMDP).

Methods

Subjects

PB specimens from a total of 306 patients with AA were analyzed for the presence of genetic alterations using SNP arrays (see Figure 1). The clinical

Submitted July 1, 2011; accepted September 18, 2011. Prepublished online as *Blood* First Edition paper, September 30, 2011; DOI 10.1182/blood-2011-07-365189.

*T.K. and A.S.-O. contributed equally to this study.

†S. Ogawa and S.N. contributed equally to this study.

The online version of this article contains a data supplement.

The publication costs of this article were defrayed in part by page charge payment. Therefore, and solely to indicate this fact, this article is hereby marked “advertisement” in accordance with 18 USC section 1734.

© 2011 by The American Society of Hematology

Table 1. Patient characteristics

	Newly diagnosed (n = 107)	Previously treated (n = 199)
Median age at diagnosis, mo (range)	64 (9-88)	24 (2-80)
Sex, male/female, no.	58/49	110/89
Severity of AA at onset, no. (%) of patients		
Severe	79 (74)	185 (93)
Nonsevere	28 (26)	14 (7)
History, mo, median (range)	19 (0.1-251)	51 (0.1-372)
Past treatment, no. (%) of patients		
ATG + CsA	—	39 (20)
CsA alone	—	51 (26)
Anabolic steroid alone	—	13 (7)
Unknown*	—	96 (48)

ATG indicates antithymocyte globulin; CsA, cyclosporine A; and —, not applicable.

*Information regarding previous therapies of 96 cases (from Japan Marrow Donor Program) was unavailable.

characteristics of these patients are summarized in Table 1 and supplemental Table 1 (available on the *Blood* Web site; see the Supplemental Materials link at the top of the online article). Among the 306 patients, 107 were newly diagnosed and 199 were previously treated. Ninety-six patients received allogeneic BM transplantation from unrelated donors through the JMDP, and their HLA information was available from the JMDP. The other 210 were newly genotyped for HLA-A, -B, -C, -DRB1, -DQB1, and -DPB1 alleles as described elsewhere.¹³ A total of 103 patients had been treated with anti-thymocyte globulin plus cyclosporine, cyclosporine alone, or anabolic steroids at the time of sampling. All patients and healthy persons provided their informed consent before sampling in accordance with the Declaration of Helsinki. The study protocol was approved by the ethics committee of the Graduate School of Medical Science, Kanazawa University and also by that of the Graduate School of Medicine, University of Tokyo.

Analysis of genomic copy numbers and detection of 6pLOH

Genomic copy numbers, as well as allele-specific copy numbers, were analyzed by using GeneChip 500K arrays (Affymetrix) as previously described.^{14,15} Briefly, genomic DNA from AA patients and normal controls were analyzed on GeneChip 500K arrays separately. After adjusting several biases introduced during experiments, signal ratios of the corresponding probes between test (patient) and controls were calculated across the genome to obtain genome-wide copy numbers. Genetic lesions, including copy number gains and losses, as well as CNN-LOHs, were first detected using a hidden Markov model-based algorithm implemented in the CNAG software.^{14,15} Known copy number variations were carefully excluded by referring to the Database of Genomic Variants (www.projects.tcag.ca/variation). CNN-LOH in 6p involving the HLA locus was more specifically and sensitively detected by statistically evaluating the mean differences in allele-specific copy numbers between heterozygous SNPs on 6p ($N = \sim 1400$) that were telomeric from the 5'-end of the HLA-A locus (rs1655927) and all non-6p heterozygous SNPs ($N = \sim 105\,000$) using the Mann-Whitney U test with the R package (www.r-project.org). Possible false-positive findings arising from multiple testing involving the 306 samples were evaluated by maintaining the false discovery rate under 0.01 as previously described,¹⁶ where the microarray data of 1000 JMDP donor specimens obtained from an ongoing whole genome association study (unpublished data) were used to calculate an empiric null distribution.^{17,18}

Determination of the missing HLA alleles in 6pLOH(+) clones in patients with AA

The 500K SNP data of the 1800 JMDP donor-recipient pairs (JMDP dataset), together with their HLA genotyping information, was used to generate an HLA SNP haplotype table on the GeneChip 500K platform, which contains the consensus SNPs of the 3 major haplotypes (P1, P2, and P3) in Japanese subjects¹⁸ and the SNP sequences of all observed HLA

haplotypes complementary to P1 to P3 within the JMDP set ($N = 1576$; data not shown). To determine the missing HLA haplotype in each 6pLOH(+) patient, those "HLA" haplotypes were first selected from the aforementioned HLA haplotype table that were compatible with the observed HLA genotypes of that patient. Among these, a candidate haplotype was selected such that it contained the minimum number of SNPs that were incompatible with the patient's genotype. For each candidate haplotype, genomic copy numbers were inferred at the heterozygous SNPs along that haplotype using the circular binary segmentation algorithm,^{19,20} which divided the haplotype into one or more discrete segments with different mean copy numbers. Finally, each copy number segment was thought to be "missing," when the alternative hypothesis ($H_a: S_i \neq \bar{S}_i$, for \forall_i) was supported against the null hypothesis ($H_0: S_i = \bar{S}_i$, for \forall_i) using the Wilcoxon signed rank test with a significance level of .05, where S_i represents the allele-specific copy number at the i th heterozygous SNP site within the segment of the candidate haplotype with \bar{S}_i being the corresponding value for the complementary haplotype (supplemental Figure 1). Finally, for those HLA types that appeared more than 8 times among 6pLOH(+) cases, their contribution to the observed allelic loss of HLA haplotypes was evaluated by multivariate logistic regression analysis with stepwise backward selection

Flow cytometry

Heparinized PB and BM were collected from the patients at diagnosis and/or after treatment. HLA-A expression on granulocytes, monocytes, B and T cells, and BM CD34⁺ cells was analyzed by flow cytometry using a FACSCanto II instrument (BD Biosciences) with the FlowJo 7.6.1 program (TreeStar). The monoclonal antibodies used for this study are provided in supplemental Table 2.

Human androgen receptor assay

The human androgen receptor gene was amplified from genomic DNA of 23 female patients, including 3 6pLOH(+) patients, as described by Ishiyama et al²¹ with some modifications. Clonality was assessed using an "S value" as a marker of skewing in granulocytes and T lymphocytes.

Association of HLA types with AA

A total of 6613 patients who had received allogeneic BM transplantation through the JMDP between 1992 and 2008 were investigated to see whether the HLA alleles frequently missing in CNN-LOH in 6p with the development of AA could represent risk alleles for the development of AA. Thus, the frequencies of patients with each of the candidate risk alleles (HLA-A*31:01, B*40:02, A*02:01, and A*02:06) and those having none of these alleles were compared between 407 patients with AA and those with other hematopoietic disorders (1827 with AML, 1606 with acute lymphocytic leukemia, 1014 with chronic myeloid leukemia, 825 with myelodysplastic syndrome, 566 with non-Hodgkin lymphoma, and 368 with other hematopoietic neoplasms; supplemental Table 3) by calculating the Fisher P values in the corresponding 2×2 contingency tables.

Results

Genetic lesions in AA detected by SNP array analysis

After excluding known or suspected copy number variations, a total of 50 genetic lesions were identified in 46 of the 306 (15%) PB specimens of our AA case series (Table 1; Figure 1). Among these by far, the most conspicuous was the recurrent CNN-LOH involving the 6p arm, which was detected in 28 cases as a significant dissociation of allele-specific copy number graphs in 6p regions using a hidden Markov model-based algorithm implemented in the CNAG software^{2,14,15} (Figure 2A-2B). Of particular interest was that all CNN-LOH in 6p commonly affected the HLA locus, causing a haploid loss of HLA alleles and uniparental HLA expression. In some cases, the breakpoint of the 6pLOH was

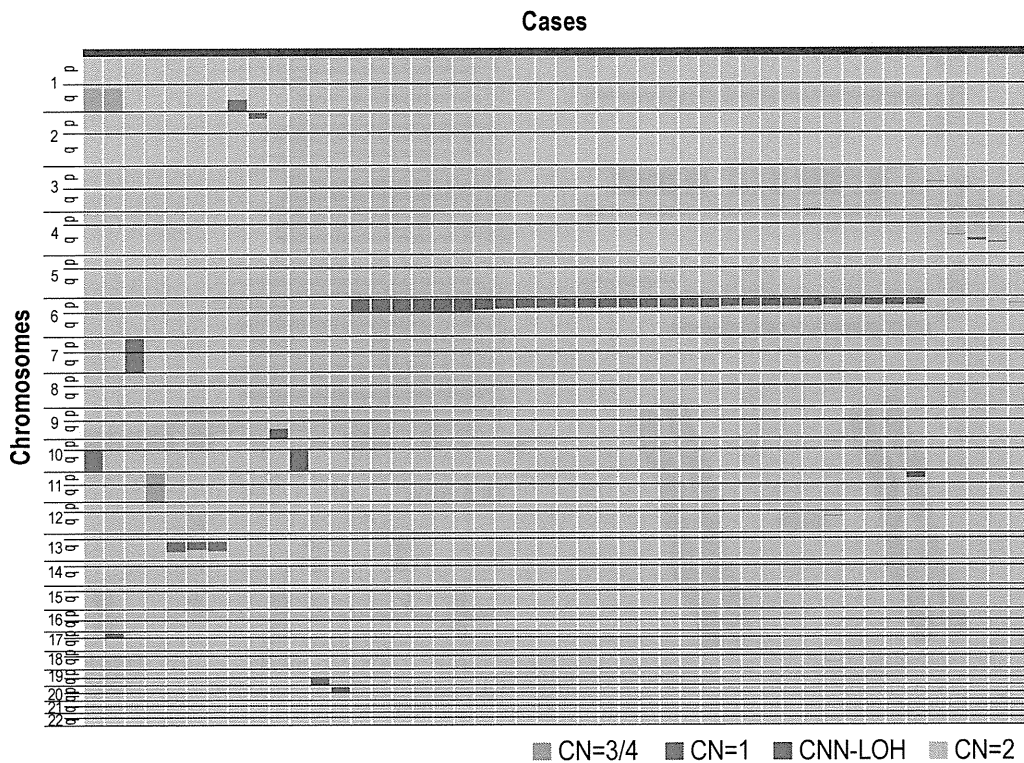


Figure 1. Copy number changes and allelic imbalances in 46 of the 306 AA cases. The copy number changes and allelic imbalances (or CNN-LOHs) in each case are summarized in the chromosomal order vertically for 46 AA cases with copy number abnormalities. Gains and losses, as well as CNN-LOHs, are shown in the indicated colors.

predicted to fall within the HLA locus (Figure 2B). These findings strongly indicated that the HLA locus was the genetic target of these 6pLOHs. Also supporting this was the finding that, in half of the cases, the dissociations in the allele-specific copy number graphs were gradually attenuated to the baseline over several mega base pair regions rather than showing a discrete breakpoint, indicating the presence of multiple 6pLOH(+) clones within a single case that had different breakpoints but still shared the same missing HLA alleles (Figure 2C). Moreover, the 6pUPDs existing only in a minor population were more sensitively detected by statistically evaluating the size of dissociation of allele-specific copy numbers in the 6p arm. With this improved statistical test, CNN-LOH in 6p was found in a total of 40 cases (13%; Figure 2D; supplemental Figure 2), where the false discovery rate was maintained at 0.01 to avoid too many false positive findings. In all 6pLOH(+) cases, substantial numbers of heterozygous SNP calls were retained within the affected regions, thus indicating that the CNN-LOHs in 6p were not constitutional but represented acquired genetic events only found in the affected subclones (Figure 1). Indeed, all 6pLOH(+) cases were shown to have “heterozygous” HLA alleles in high-resolution HLA typing of their PB (Table 2). Moreover, 6pLOH was not detected in the CD3-positive T cells in selected cases (cases 25 and 26, supplemental Figure 3). By quantitatively comparing the observed differences in allele-specific copy numbers in the 6pLOH segments with what were expected assuming 100% LOH(+) components, the 6pLOH(+) clones were estimated to account for 0.2% to 53.9% of the PB leukocytes (Table 2). The trend of the lower percentages of the 6pLOH(+) fraction in newly diagnosed patients compared with those in patients at remission was thought to reflect the fact that the former patients tended to have lower counts of granulocytes and monocytes, which

were the predominant targets of 6pLOH (see supplemental Table 1).

The disease status of the 40 patients at the sampling was before treatment in 16 cases, during remission for 1 to 16 years after therapies in 15, and before BM transplantation for refractory disease in 9. All evaluable 6pLOH(+) AA cases responded to immunosuppressive therapy (IST) (23 of 23), whereas 101 of 126 evaluable cases with 6pLOH(−) responded ($P = .014$; Table 3).

Uniparental expression of HLA-A in multilineage hematopoietic cells

The genetic loss of one HLA haplotype in SNP array analysis was further confirmed by expression analysis of HLA-A in PB leukocytes using flow cytometry in 19 eligible cases with 6pLOH(+), in which the HLA-A alleles were heterozygous and fresh PB samples were available. Loss of expression of one HLA-A antigen was confirmed in all 19 6pLOH(+) cases (Figure 3A; supplemental Figure 4). The HLA-A missing cells in the PB were shown to have appeared shortly after the onset or before the initiation of treatments in 2 cases, and were confirmed to persist for 1 to 16 months (median, 6 months) in 14 patients (supplemental Table 1; supplemental Figure 5). The percentage of granulocytes lacking HLA-A antigens in the 2 patients who were responsive to IST remained almost the same during the convalescent period of 2 to 3 months (supplemental Figure 6). Importantly, uniparental expression of HLA-A alleles was detected in multiple cell lineages, including granulocytes, monocytes, B cells, and, to a lesser extent, in T cells. Moreover, uniparental HLA-A expression was demonstrated in BM CD34+ cells in 5 patients whose BM samples were available for flow cytometry. All 5 patients possessed various proportions of BM CD34+ cells (49.7%-71.3%), which had lost the expression of one